



Emissions of volatile organic compounds (VOCs) from gasoline- and liquified natural gas (LNG)-fueled vehicles in tunnel studies

Congbo Song¹, Yan Liu, Luna Sun, Qijun Zhang, Hongjun Mao*

Tianjin Key Laboratory of Urban Transport Emission Research & State Environmental Protection Key Laboratory of Urban Ambient Air Particulate Matter Pollution Prevention and Control, College of Environmental Science and Engineering, Nankai University, Tianjin 300071, China

HIGHLIGHTS

- Inconsistent fleet-average VOC emissions due to different fleet compositions.
- Real-world VOC emissions from gasoline vehicles (GVs) were measured in two tunnels with >94% GV in the fleets.
- Constrained linear regression was used to distinguish VOC emissions from LNG-fueled vehicles and GV.
- Fleet-average emission factors of VOCs substantially decreased over the last decade.
- Aromatics and alkenes dominated VOC reactivity from gasoline- and LNG-fueled vehicles, respectively.

ARTICLE INFO

Keywords:

Volatile organic compounds
Gasoline vehicles
Liquified natural gas
Emission factor
Source profile
Tunnel study

ABSTRACT

Gasoline vehicles (GVs) emissions generally dominate ambient volatile organic compounds (VOCs) in urban areas, while VOC emissions from liquefied natural gas (LNG)-fueled vehicles play an increasingly important role in urban air quality, due to fuel transition from gasoline/diesel to alternative fuels. Here, an extensive dataset of VOC samples collected in three urban tunnels in China was used to explore real-world emission characteristics of ninety-nine VOC species from both GV and LNG-fueled vehicles. The fleets in the Beijing and Tianjin tunnels comprised >94% GV whereas the fleet in the Nanjing tunnel comprised both GV (~87%) and LNG-buses (~13%). The VOC emission factors (EFs) in the Beijing tunnel and Tianjin tunnel were highly correlated, implying that they can be applied as existing emission datasets from GV with aim of distinguishing emissions from LNG-fueled vehicles and GV in the Nanjing tunnel. For fleet emissions, the average VOC EFs have declined substantially over the last decade; the relative compositions of benzene, toluene, and ethylbenzene were quite stable despite differences in fleet composition. Ethylene, isopentane, ethane, and toluene; and ethane and propane were enriched in VOC emissions (*v/v*) from GV and LNG-fueled vehicles, respectively. Methyl *tert*-butyl ether, 2,2,4-trimethylpentane, 2,3,4-trimethylpentane, 3-methylpentane, and methylcyclopentane were potential VOC tracers for GV. Ethane, propane, and 2,3-dimethylbutane were key tracers that distinguished LNG-fueled vehicles from GV. Propane, isobutane, and *n*-butane were key VOC tracers that distinguished liquefied petroleum gas-fueled vehicles from GV. Alkanes dominated fleet emissions both by mass and by volume. However, aromatics and alkenes (mainly ethylene and propylene) dominated VOC reactivity from gasoline- and LNG-fueled vehicles, respectively. Our study highlights that the wide discrepancy in fleet VOC emissions could be attributed to fleet compositions.

1. Introduction

Volatile organic compounds (VOCs) are ubiquitous organic pollutants in the ambient atmosphere. Critical roles of ambient VOCs mainly include: (1) the toxicity of many species and resulting adverse health effects and (2) participation in atmospheric reactions that contributes to

the formation of tropospheric ozone (O₃) and secondary organic aerosol (SOA). To develop efficient abatement strategies of VOC emissions, improve air quality and ensure public health, refined emission inventory (i.e., source method) or source apportionment (i.e., receptor method) of VOCs is often required. Determination of emission factors (EFs) of speciated VOCs from various sources (i.e., anthropogenic and biogenic

* Correspondence to: College of Environmental Science and Engineering, Nankai University, Tianjin 300071, China.

E-mail address: hongjunm@nankai.edu.cn (H. Mao).

¹ Now at: School of Geography, Earth and Environmental Sciences, University of Birmingham, Birmingham, B15 2TT, United Kingdom.

emissions) is essential for both reliable emission inventories and source apportionment studies.

The main anthropogenic source of ambient VOCs in urban areas is typically traffic-related emissions (Song et al., 2019; Brown et al., 2007; Vega et al., 2000), including tailpipe emissions, evaporative emissions, and liquid/unburned fuel. In general, emissions of gasoline vehicles (GVs) contribute most of the VOCs in urban atmosphere (Parrish et al., 2009), while diesel vehicles (DVs) dominate vehicle emissions for PM_{2.5} and NO_x (Song et al., 2018). Nowadays VOC emissions from liquefied natural gas (LNG)-fueled vehicles play an increasingly significant role in urban air quality (Zhang et al., 2018c; Li et al., 2017; Huang et al., 2015) because of transition from conventional fuels to alternative-fuels on account of their potential capability of reducing emissions of air pollutants compared with GV and DVs. Natural gas (NG), suggested to be a cheaper and cleaner fuel than gasoline and diesel, is the fastest-growing form of transportation energy use. Starting from much lower levels of use than liquid fuels, these have become a promising alternative fuel for use in engines of taxis and buses because of their potential demands of high trip mileage. In addition, the storage of natural gas resources has been greatly expanding thanks to advances in horizontal drilling and hydraulic fracturing technologies. Therefore, it is imperative to understand the magnitude and characteristics of VOC emissions from gasoline- and LNG-fueled vehicles, which were the largest sources of VOC emissions from on-road vehicles.

Measurement of vehicular VOC emissions is resource intensive, and generally involves chassis dynamometer testing (Wang et al., 2013; Guo et al., 2011; Schmitz et al., 2000), portable emission measurement system (PEMS) (Wang et al., 2020; Cao et al., 2016; Yao et al., 2015a), sealed housing for evaporative determination (SHED) (Man et al., 2020; Yue et al., 2017; Yamada, 2013; Zhang et al., 2013), and tunnel testing (Zhang et al., 2018a; Stemmler et al., 2005). In general, tailpipe and evaporative emissions from individual vehicles are determined by dynamometer testing and SHED, respectively. However, the limitations of dynamometer testing and SHED are: (1) small sample numbers for individual testing; (2) simulated driving conditions rather than real-world conditions; (3) representing only tailpipe emissions or evaporative emissions from individual vehicle; and (4) not accurate estimation on the dilution of VOCs. Tunnel test can be an excellent approach to overcome these limitations and estimate primary vehicular VOC emissions including both tailpipe and evaporative emissions from a fleet under real-world driving conditions (Hampton et al., 1982, 1983). Tunnel tests have been extensively used to measure speciated VOC source profiles and EFs from fleet emissions, such as in Taiwan (Hung-Lung et al., 2007; Hwa et al., 2002), Hong Kong (Cui et al., 2018; Ho et al., 2009), Guangzhou (Zhang et al., 2018c; Fu et al., 2005), and Nanjing (Zhang et al., 2018a). In addition, some studies conducted repeated measurements at a same tunnel to assess the effectiveness of local vehicular emission control strategies and/or new technologies to reduce vehicular VOC emissions (Cui et al., 2018; Zhang et al., 2018c; Stemmler et al., 2005). Despite huge research interest and many contributions over the last decades, it is quite a challenge to narrow the uncertainties in VOC EFs and source profiles of vehicular emissions in tunnel tests. This is mainly because of a great diversity of fleet compositions and the transition from gasoline/diesel to alternative fuels. For example, inconsistent decreasing percentages of fleet-average VOC EFs were observed in Cui et al. (2018)'s study in Hong Kong (i.e., 45% from 2003 to 2015) and Zhang et al. (2018c)'s study in Guangzhou (i.e., only 9% from 2004 to 2014); markedly higher fleet-average VOC EFs ($\mu \pm \sigma$) was found in Zhang et al. (2018a)'s study in Nanjing in 2015 (i.e., $174.39 \pm 16.86 \text{ mg km}^{-1} \text{ veh}^{-1}$) and Zhang et al. (2018c)'s study in Guangzhou in 2014 (i.e., $449 \pm 40 \text{ mg km}^{-1} \text{ veh}^{-1}$) than that in Cui et al. (2018)'s study in Hong Kong in 2015 (i.e., $58.8 \pm 50.7 \text{ mg km}^{-1} \text{ veh}^{-1}$) though these tunnel tests were conducted in similar years. The wide discrepancy in fleet-average EFs could introduce substantial uncertainties in establishing emission inventories even at a city-level (Wang et al., 2018; Song et al., 2018).

The breakdown of a mixed fleet into fuel-specific vehicle types could be worthwhile because of the possibility of narrowing the uncertainties and the broader applicability in bottom-up emission inventories and refined source apportionment studies. A number of studies have been able to differentiate emissions from GV and DV (Cui et al., 2016; Pierson et al., 1983), light-duty vehicles (LDV) and heavy-duty vehicles (HDV) (Legreid et al., 2007; Stemmler et al., 2005; Colberg et al., 2005), heavy-duty diesel vehicles (HDDVs) and non-HDDVs (Song et al., 2018), by linear regression between fleet-average EFs and proportion of a vehicle type in the fleet. In general, incorporating *prior* information of EFs from one vehicle type into the linear regression could substantially reduce the uncertainty of the breakdown. EFs from GV could be easily measured, since GV dominate vehicle population in China with a proportion of ~88.7% in 2018 (MEEPRC, 2019). In megacities in northern China, such as Beijing and Tianjin, the proportion of GV in urban fleets could be >90% since heavy/medium-duty diesel vehicles are often restricted in urban areas (Song et al., 2018). Therefore, tunnel tests in urban areas in Beijing and Tianjin gave us a unique opportunity to measure VOC emissions from GV under real-world driving conditions. In addition, we also conducted a tunnel test in Nanjing in eastern China, a tunnel that has been reported in previous studies (Zhang et al., 2018a; Chen et al., 2013). Owing to the full implementation of the LNG fuel in buses in Nanjing since 2005, the fleet in the Nanjing tunnel in 2015 comprised ~87% GV and ~13% LNG-buses (Zhang et al., 2018a), which was obviously different with those in the Beijing tunnel and Tianjin tunnel. The distinct fleet compositions of those tunnels allowed the source signatures to be resolved and the EFs of VOCs from both gasoline and LNG-fueled vehicles to be estimated.

In the present study, an extensive dataset of VOC samples collected in three urban tunnels from 2015 to 2017 were analyzed, to offer a comprehensive understanding of emission characteristics of ninety-nine VOC species from both GV and LNG-fueled vehicles under real-world driving conditions. The obtained data and analysis point towards future studies, including quantifying contributions of vehicular emissions to ambient VOCs in multi-scale atmospheric environment using tracer-based approach, incorporating the source profiles into advanced receptor models like constrained-positive matrix factorization (PMF), apportioning fleet VOC emissions to tailpipe and evaporative emissions, and establishing VOC emission inventories and evaluating air quality modeling.

2. Materials and methods

2.1. Tunnel tests and instruments

The basic information about the tunnels, sampling protocol, traffic, and meteorology is summarized in Table 1:

- (i) –*Beijing*. Dongguan Tunnel ($116^{\circ}39'33''\text{E}$, $39^{\circ}55'2''\text{N}$) is an urban tunnel located in Tongzhou district in Beijing city. The fleet in the tunnel was dominated by GV (98%), due to a height limit of 3.5 m and a restriction of heavy-duty trucks (HDTs) in the tunnel. The average speed in the tunnel was $40.3 \pm 5.3 \text{ km h}^{-1}$ with a speed limit of 50 km h^{-1} . During the test period, $15,592 \pm 248$ vehicles traveled through per day, the average temperature was $22.7 \pm 3.4^{\circ}\text{C}$ during the tunnel test. VOC samples (24 in total) were collected on 4 samples/d with 3-h intervals (00:00–03:00, 06:30–09:30, 11:00–14:00, and 16:00–19:00 LT) both in the inlet and outlet of the tunnel on 24–26 September 2017.
- (ii) –*Tianjin*. Wujinglu Tunnel ($117^{\circ}12'15''\text{E}$, $39^{\circ}8'31''\text{N}$) located in the central urban area of Tianjin. The vehicle speed limit in the tunnel was 40 km h^{-1} , and the average daily traffic volume was $14,866 \pm 900$ vehicles. The fleet in the tunnel primarily comprised light-duty passenger vehicles (LDPVs), accounting for $96.3 \pm 0.7\%$ of the total vehicles. GV were the most common

Table 1
Basic information about the tunnels, sampling, traffic, and meteorology.

Tunnel test	Dongguan Tunnel, Beijing	Wujinglu Tunnel, Tianjin	Fu Gui Mountain Tunnel, Nanjing
<i>Tunnel parameters</i>			
Tunnel type	Urban tunnel	Urban tunnel	Urban tunnel
Latitude	116° 39'33"E	117° 12'15"E	118° 48'52"E
Longitude	39° 55'2"N	39° 8'31"N	32° 3'25"N
Tunnel length (m)	905	1500	480
Cross-sectional area (m ²)	58	54	65
Speed limit (km h ⁻¹)	50	40	50
<i>Sampling</i>			
Sampling site	Inlet & Outlet	Inlet & Outlet	Inlet & Outlet
Inlet/Outlet site (m) ^a	30/700	45/605	20/460
Sampling height (m)	1.5	1.5	0.5
Sampling period	24–26/09/2017	10–11/08/2017	20–23/06/2015
Sampling time	00:00–24:00	00:00–24:00	07:00–21:00
Duration per sample (h)	3	3	4
Number of samples	24	28	24
<i>Traffic and Meteorology</i>			
Traffic volume (veh d ⁻¹)	15,592 ± 248	14,866 ± 900	6000 ^b
Fleet-average speed (km h ⁻¹)	40.3 ± 5.3	35.6 ± 1.7	44.2
Fleet composition	98% GVs	94% GVs, 2% DVs	87% GVs, 13% LNG
Outlet temperature (°C)	24.1 ± 3.6	29.7 ± 1.6	(21.2–26.5)
Outlet relative humidity (%)	39.4 ± 16.0	61.8 ± 8.9	(63.0–88.3)
Outlet wind speed (m s ⁻¹)	1.4 ± 0.5	0.8 ± 0.3	(1.4–1.8)

^a: the sampling site denotes the distance between the sampling site and the tunnel entrance.

^b: the average traffic volume during 07:00–21:00.

in the fleet (94.2 ± 0.3%). Alternative-fuel (compressed natural gas: CNG, LNG, liquefied petroleum gas: LPG, electronic, and hybrid) vehicles were emerging which accounted for nearly 3.8 ± 0.3% of the total vehicles, and were almost twice as common as DVs (2.0 ± 0.3%). The average temperature was 29.3 ± 3.0°C during the tunnel test. VOC samples (28 in total) were collected on 7 samples/d with 3-h intervals (00:00–03:00, 06:00–09:00, 09:00–12:00, 12:00–15:00, 15:00–18:00, 18:00–21:00, and 21:00–24:00 LT) both in the inlet and outlet of the tunnel on 10–11 August 2017.

- (iii) –Nanjing. Fu Gui Mountain Tunnel (118°48'52"E, 32°3'25"N), in the eastern Nanjing, passes through the Fu Gui Mountain in the Xuanwu District in Nanjing city. Base on radio-frequency identification (RFID) data, vehicle speeds ranged from 41.6 to 45.8 km h⁻¹. The average daily traffic volume was approximately 9000 vehicles. The fleet in the Nanjing tunnel comprised 87 ± 3% GVs and 13 ± 3% LNG-buses. During the test, the temperatures of the inlet and outlet were 22.3–29.8 °C and 23.9–30.8 °C, respectively. VOC samples (24 in total) were collected on 3 samples/d with 4-h intervals (7:00–11:00, 12:00–16:00, and 17:00–21:00 LT) both in the inlet and outlet of the tunnel on 20–23 June 2015.

3.2-L pre-evacuated stainless-steel canisters (Entech Instruments, Inc., Simi Valley, CA, USA) were used throughout the above tunnel tests. The constant flow rate of the canisters was controlled by CS1200E (Entech Instruments, Inc., Simi Valley, CA, USA), a flow controller for time integrated sampling (i.e., duration per sample). Meteorological data including temperature, relative humidity, and wind speed in the outlet of the tunnels were measured by VAISALA WXT520 (Helsinki, Finland) automatic weather stations. The actual volumetric flow rates induced by the vehicular fleet and the prevailing winds in the Tianjin and Nanjing were continuously measured using ultrasonic flowmeters (Flowsick-200 SICK MAIHAK, Germany). Traffic counts and vehicle speed during tunnel tests in Beijing and Tianjin were continuously monitored using roadside laser loop detectors (AxleLight RLU11) that were installed at the outlet of the tunnels. In addition, the license plates of vehicles passing through the Beijing and Tianjin tunnels were captured by high-definition vehicle license plate recognition system. The vehicle classification results for these two tunnels were obtained by matching

the license plates and registered vehicle database. The detailed traffic counts, vehicle speed, and vehicle classification in the Nanjing tunnel were obtained from radio-frequency identification (RFID) system.

2.2. Laboratory analysis and QA/QC

All samples were analyzed using high-performance gas chromatography combined with a mass spectrometer system and flame ionization detector (GC–MS/FID, TH-PKU 300B, Wuhan Tianhong Instruments Co. Ltd., Wuhan, China). Ninety-nine VOC species were quantified by the system. These include 29 alkanes, 11 alkenes, 1 alkyne, 16 aromatics, 28 halocarbons, and 14 oxygenated VOCs (OVOCs). The system has two channels and dual detectors. 300 mL of each sample was drawn through a cryogenic trap at a flow rate of 60 mL min⁻¹, and cooled to –160 °C for pre-concentration. CO₂ and moisture are removed before injection. After being trapped, the lash concentrated VOCs were flash desorbed by heating at 100 °C and transferred to the chromatographic column. Separation used a carrier gas (high-purity helium). C2–C5 hydrocarbons were separated on a PLOT-Al₂O₃ columns (15 m × 0.32 mm × 6.0 μm) and detected by an FID, while C5–C12 hydrocarbons were separated on a DB-624 column (60 m × 0.25 mm × 1.4 μm) and detected by an MS. The initial temperature for the chromatographic column was 41 °C, maintained for 6 min, and then raised to 180 °C at a rate of 6 °C min⁻¹. The detectors and method detection limits (MDLs) for each VOC species are listed in Table S1.

All canisters were cleaned (Entech 3100 Canister Cleaning Systems, Entech Instruments, Inc., Simi Valley, CA, USA) by using high-purity nitrogen (N₂) and vacuumed (<0.05 mm Hg) before sampling. The chemical analysis of tunnel samples was completed within 36 h after sampling. The quantification of VOCs was performed by internal and external standard methods. Standard gas mixtures (Scott Specialty Gases, USA) of PAMS (photochemical assessment monitoring stations) and TO-15 (Toxic Organics-15) species were used as external standards for 5-point calibrations. The correlation coefficients usually were usually >0.99 (Table S1). Additionally, bromochloromethane, 1,4-difluorobenzene, chlorobenzene, and 4-bromofluorobenzene were used as internal standards for calibration. During the sample analysis, 2 ppbv of the standard VOCs gas were used as daily calibration to check the system stability.

2.3. Fleet-average primary emissions

For each VOC species, the corresponding inlet concentrations were subtracted from the outlet values ($\Delta C_{\text{con.}}: C_{\text{Outlet}} - C_{\text{Inlet}}$) to gain the emission signals from vehicles traveling through the tunnel. The fleet-average VOC source profiles, defined as relative abundances ($v/v\%$) of speciated VOCs, in tunnel studies were calculated as follows:

$$\text{Percentage}_{i,j} = \frac{C_{i,j-\text{Outlet}} - C_{i,j-\text{Inlet}}}{\sum_{n=1}^N (C_{n,j-\text{Outlet}} - C_{n,j-\text{Inlet}})} \times 100\% \quad (1)$$

where $\text{Percentage}_{i,j}$ is the percentage of VOC species i in paired-sample j ; $C_{i,j-\text{Inlet}}$ and $C_{i,j-\text{Outlet}}$ are concentrations (ppbv) of VOC species i at the inlet and outlet of paired-sample j , respectively. N is the number of VOC species measured.

The fleet-average EFs for vehicles traveling through the tunnel were estimated using the following formula (Song et al., 2018; Fang et al., 2019; Zhang et al., 2018a; Gertler et al., 1996; Pierson et al., 1996; Pierson and Brachaczek, 1983).

$$EF_{i,j} = \frac{(C_{i,j-\text{Outlet}} - C_{i,j-\text{Inlet}}) \times M_i \times A \times v \times T}{1000 \times V_m \times N \times L} \quad (2)$$

where, $EF_{i,j}$ ($\text{mg km}^{-1} \text{veh}^{-1}$) is the fleet-average emission factor in paired-sample j for species i . M_i (g mol^{-1}) is the relative molecular mass of the VOC species i . A (m^2) is the cross-section area of the tunnel. v (m s^{-1}) is the air velocity parallel to the tunnel measured by the ultrasonic gas flowmeters or automatic weather stations. V_m is the standard molar volume (i.e., 22.4 L mol^{-1}). N (veh) is the traffic count traveling through the tunnel during the time intervals T (s) of each paired-sample. L (km) is the distance between the inlet site and outlet site.

For EFs ($\text{mg km}^{-1} \text{veh}^{-1}$) extracted from other tunnel tests in published literatures, the source profiles ($v/v\%$) could be obtained using the following formula:

$$\text{Percentage}_i = \frac{EF_i/M_i}{\sum_{n=1}^N (EF_n/M_n)} \times 100\% \quad (3)$$

2.4. Breakdown of fleet-average EFs

Linear regression between the fleet-average EFs and traffic composition (i.e., proportion of a specific vehicle type in the fleet) would be the best approach to calculate average EFs for two principle vehicle types (i.e., type 1 and type 2), as:

$$EF_{i,j} = EF_{i,j,1} \times pV_{j,1} + EF_{i,j,2} \times (1 - pV_{j,1}) + \epsilon \quad (4)$$

where $EF_{i,j}$ ($\text{mg km}^{-1} \text{veh}^{-1}$) is the fleet-average emission factor in a paired-sample j for species i ; $EF_{i,j,1}$ and $EF_{i,j,2}$ ($\text{mg km}^{-1} \text{veh}^{-1}$) are the EFs of vehicle type 1 and 2, respectively. $pV_{j,1}$ and $pV_{j,2}$ are the proportions of the vehicle type 1 and 2 in the fleet during the paired-sample j , respectively. ϵ is the random error.

The linear regression model requires that significant variation in fleet composition are available. Otherwise it could fail to apportion the fleet-average EFs into different vehicle types. In our case, the Beijing and Tianjin fleets mainly comprised GVVs (>94%), while the Nanjing fleet comprised both GVVs ($87 \pm 3\%$) and LNG-buses ($13 \pm 3\%$). The EFs of VOCs from LNG-fueled vehicles in the tunnel test in Nanjing could be quantified by constraining the EFs of GVVs in the Beijing and Tianjin fleets, as follows (rewritten form of Eq. (4)):

$$EF_{i,j,\text{LNG}} = \frac{EF_{i,j} - (1 - pV_{j,\text{LNG}}) \times EF_{i,\text{GVs}}}{pV_{j,\text{LNG}}} + \epsilon \quad (5)$$

where, $EF_{i,\text{GVs}}$, the average EF of species i from GVVs, is derived and adjusted from fleet-average EF in the Beijing tunnel and Tianjin tunnel. $pV_{j,\text{LNG}}$ is the proportion of the LNG-buses in the fleet during the paired-sample j . The $pV_{j,\text{LNG}}$ ranged from 7.3% to 17.3%, with an average value of $13 \pm 3\%$ (Table S2).

It should be noted that the average EFs of GVVs in the Beijing and Tianjin tunnels in 2017 need to be adjusted to 2015 when the Nanjing tunnel study was performed to reduce the uncertainties in applying Eq. (5) induced by the inconsistent test year of the tunnel tests. There are two basic assumptions to ensure that the adjustment is reasonable:

Assumption 1. The VOC source profile of GVVs has not substantially changed from 2015 to 2017. The China IV and China V emission standards were implemented in July 2011 and January 2017, respectively. From China IV to China V standard, the limits of benzene and aromatics remain unchanged, and the limit of alkenes only decreased from 28% to 24%. During the tunnel test in Tianjin in 2017, China I, China II, China III, China IV, and China V accounted for 0.7%, 4.1%, 19.0%, 48.5%, and 27.8% of GVVs. China IV dominated the GVVs both in Nanjing in 2015 (36.2%) and in Beijing/Tianjin in 2017 (48.5%), though China V emission standards had been implemented in January 2017. This might be due to the fact that the number of new vehicle registration (China V) is lower than that of the existing vehicles with China IV by September 2017. Therefore, Assumption 1 is reasonable, and EFs of speciated VOC for GVVs in 2015 can be estimated using the following formula:

$$EF_{i,2015} = \frac{EF_{\text{BTEX},2015}}{EF_{\text{BTEX},2017}} \times EF_{i,2017} \quad (6)$$

where $EF_{i,2015}$ and $EF_{i,2017}$ ($\text{mg km}^{-1} \text{veh}^{-1}$) are the average EFs for species i in 2015 and 2017, respectively. $EF_{\text{BTEX},2015}$ and $EF_{\text{BTEX},2017}$ are the average EFs for BTEX (i.e., the sum of benzene, toluene, ethylbenzene, *m*, *p*-xylene, and *o*-xylene) in 2015 and 2017, respectively. The $EF_{\text{BTEX},2017}$ can be obtained from tunnel studies in the Beijing and Tianjin tunnels that were conducted in 2017. We used BTEX species instead of C2-C5 species to calculate $EF_{i,2015}$ because (1) the limits of benzene and aromatics remain unchanged from China IV to China V; (2) the relative compositions of benzene, toluene, and ethylbenzene were relatively stable despite differences in fleet composition (will be discussed later); (3) C2-C5 species are often observed as VOC tracers for different fuels (e.g., gasoline/LNG/LPG); and (4) BTEX species have been measured broadly in the previously studies.

Assumption 2. The EFs of VOCs from GVVs declined gradually over the past decade. There are studies that noted that large decrease of VOC emissions from urban fleets over the past years (Zhang et al., 2018a; Cui et al., 2018; Zhang et al., 2018c; Stemmler et al., 2005), due to newly registered vehicles with stringent emission standards, and improved engine technologies. Assumption 2 is also reasonable because the fleet structure changed gradually with elimination of older vehicles and the addition of new ones since the introduction of new emission standards (Sun et al., 2019). Therefore, the $EF_{\text{BTEX},2015}$ for GVVs can be estimated using the equation below:

$$EF_{\text{BTEX},2015} = EF_{\text{BTEX},2017} + (2015 - 2017) \times k \quad (7)$$

where k ($\text{mg km}^{-1} \text{veh}^{-1} \text{yr}^{-1}$) is the slope of linear regression between EF_{BTEX} and the test years.

Combining Eqs. (5)–(7), the EFs of speciated VOCs from LNG-buses could be approximately estimated.

2.5. Chemical reactivity of vehicular VOCs

The kinetic reactivity and mechanism reactivity of the VOCs are widely used to understand the role of VOCs in O_3 formation (Song et al., 2019; Liu et al., 2016; Zou et al., 2015). The kinetic reactivity of the VOCs was estimated by their propylene-equivalent (Propy-Equiv) emissions.

$$E_{i,\text{Propy-Equiv}} = E_{i,V} \times C_i \times \frac{k_{i,\text{OH}}}{k_{\text{Propy},\text{OH}}} \quad (8)$$

where i is a VOC species, $E_{i,\text{Propy-Equiv}}$ ($\text{ml km}^{-1} \text{veh}^{-1}$) is the Propy-Equiv EF. $E_{i,V}$ is the EF by volume ($\text{ml km}^{-1} \text{veh}^{-1}$). C_i is the number of

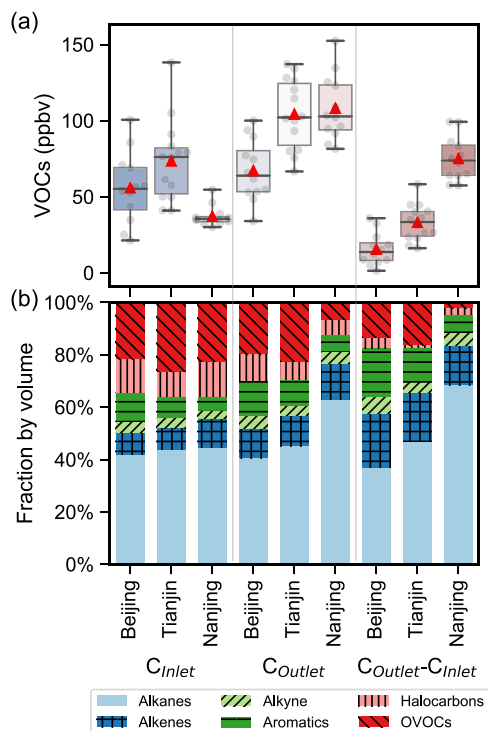


Fig. 1. (a) Boxplots (mean values were denoted as triangles) of total measured VOCs and (b) fractions of VOC groups (i.e., alkanes, alkyne, aromatics, halocarbons, and OVOCs) in tunnel samples (i.e., C_{Inlet} , C_{Outlet} , and $C_{Outlet}-C_{Inlet}$) in the Beijing, Tianjin, and Nanjing tunnels.

carbon atoms. $k_{i,OH}$ and $k_{Propyl,OH}$ represent the chemical reaction rate constants in the free radical reaction of species i and propylene with OH, respectively. $k_{i,OH}$ was obtained from Atkinson and Arey (2003). $E_{i,V}$ can be calculated with:

$$E_{i,V} = \frac{EF_i \times V_m}{M_i} \quad (9)$$

The mechanism reactivity of the VOCs was estimated by their maximum-incremental-reactivity (MIR) weighted emissions (the maximum concentration of O_3 generated by the species in terms of estimated MIR).

$$E_{i,OFP} = EF_i \times MIR_i \quad (10)$$

where $E_{i,OFP}$ ($mgO_3 \text{ km}^{-1} \text{ veh}^{-1}$) is the ozone formation potential (OFP) of VOC species i , MIR_i ($g \text{ g}^{-1}$) is the maximum incremental reactivity coefficient for VOC species i from previous studies (Carter, 1994; Dodge, 1984).

3. Results and discussion

3.1. VOC concentrations and compositions

The VOC concentrations and group compositions in the tunnel tests are presented in Fig. 1. The average concentrations of total measured VOCs at the inlet of Beijing, Tianjin and Nanjing tunnels were 55.9 ± 23.4 ppbv, 73.5 ± 26.7 ppbv, and 37.2 ± 6.8 ppbv, respectively. The average concentrations of the total measured VOCs at the outlet of Beijing, Tianjin, and Nanjing were 67.2 ± 20.1 ppbv, 104.3 ± 23.1 ppbv, and 108.2 ± 21.5 ppbv, respectively. The $\Delta Con.$ represents the absolute contribution of vehicular emissions to VOC concentrations when passing through the tunnel. The $\Delta Con.$ in Beijing, Tianjin, and Nanjing tunnel were 15.6 ± 10.7 ppbv, 33.1 ± 11.8 ppbv, and 75.1 ± 14.5 ppbv, respectively. According to Eq. (2), $\Delta Con.$ were affected by four factors:

fleet-average EFs, tunnel parameters (length, cross section area, etc.), traffic volume, and air velocity.

Fig. 1b shows relative fractions of VOC groups in the tunnel tests. For C_{Inlet} , C_{Outlet} , and $\Delta Con.$, alkanes were the most abundant group throughout the tunnel tests. Alkanes were reported as the dominant VOC group in ambient measurements in major Chinese cities (Song et al., 2019), which could be attributed to high emissions of alkanes from vehicles and natural gas sources. For the Beijing and Tianjin tunnels, the VOC composition at the inlet and outlet site were similar, with R^2 of 0.97. This indicated that vehicular emissions were the dominant VOC sources at both sites and consistent with previous studies (Cui et al., 2018; Ho et al., 2009). Unlike the Beijing and Tianjin tunnels, markedly different VOC compositions were found at the inlet and outlet of the Nanjing tunnel, likely due to much a higher proportion of bus in the tunnel fleet (13.8%) than that in the urban fleet (6%) (Zhang et al., 2018b).

On average, alkanes, alkenes, alkyne, aromatics, halocarbons, and OVOCs accounted (by volume) for, respectively, 36.8%, 20.6%, 6.5%, 18.7%, 3.9%, and 13.5% in Beijing; 47.0%, 18.7%, 3.9%, 13.3%, 0.9%, and 16.3% in Tianjin; and 68.4%, 15.1%, 4.8%, 7.0%, 2.5%, and 2.1% in Nanjing. A higher abundance of alkanes in Nanjing was observed compared to Beijing and Tianjin, mainly due to a greater proportion of LNG-buses in the Nanjing tunnel. Zhang et al. (2018c) also reported that alkanes accounted for as high as $58.1 \pm 2.6\%$ of the total VOCs in the Guangzhou Tunnel in 2014, which was mainly attributed to 27% LPG-fueled vehicles in the fleet. Thus, alkanes were the most abundant group (36.8–68.4%) in vehicular VOC emissions, especially for fleets with higher proportions of LNG/LPG-fueled vehicles. Additionally, alkanes are expected to continue to dominate vehicular VOC emissions since the limits (GB 17930–2016) of alkenes and aromatics in gasoline decrease from China V (alkenes limit: 24%; aromatics limit: 40%) to China VI (alkenes limit: 18%; aromatic limit: 35%) (AQSIQ, 2017), and promotion of NG/LPG-fueled vehicles.

3.2. Diagnostic ratios of vehicular emissions

Diagnostic ratio (v/v) of pair species (the slope of correlation plot) is often used either to identify potential emission sources (Song et al., 2019; Zhang et al., 2016; Steinbacher et al., 2005; Hedberg et al., 2002) or as a chemical clock for determination of photochemical age of air masses (Yuan et al., 2012; Nelson and Quigley, 1983). Among the VOC species, toluene (T) and benzene (B), ethylbenzene (E) and *m,p*-xylene (X), isobutane (*i*-Bu) and *n*-butane (*n*-Bu), and isopentane (*i*-P) and *n*-pentane (*n*-P); are often found to be well correlated in ambient measurements (Song et al., 2019; Zheng et al., 2018; Khoder, 2007) as well as in tunnel studies (see Fig. 2).

The vehicular T/B ratios (Fig. 2a) were 2.5 (95% CI: 1.7, 3.9) in Beijing, 1.1 (95% CI: 0.9, 1.4) in Tianjin, 2.3 (95% CI: 1.9, 2.9) in Nanjing and 1.0 (95% CI: 0.8, 1.3) in these three tunnel tests. The vehicular T/B ratios measured in Beijing and Nanjing were approximately twice that measured in Tianjin. On January 1, 2017, Beijing implemented a stricter benzene limit (0.8%, DB11/238-2016) on supplied gasoline with benzene content lower than national limit (1%, GB17930-2016), leading to a higher vehicular T/B ratio than that in other cities. The higher vehicular T/B ratio in Nanjing was likely due to the high proportion of LNG-buses in the fleet, since it was similar to those measured in Guangzhou in 2014 (T/B: ~ 2.0 , v/v) and in Hong Kong in 2015 (T/B: ~ 3.5 , v/v), which were characterized by LPG-fueled vehicles. Our tunnel tests suggested a T/B ratio of 1.0 (95% CI: 0.8, 1.3) could be used as a constraint for vehicular emissions when conducting receptor modeling. The results were consistent with reported diagnostic ratios, which were 1–10 for vehicular emissions (Zhang et al., 2016; Liu et al., 2008). However, it could be a challenge to identify vehicular emissions based on T/B ratios that were measured in the ambient, since the T/B ratios for vehicular emissions overlap with other sources (Zhang et al., 2016).

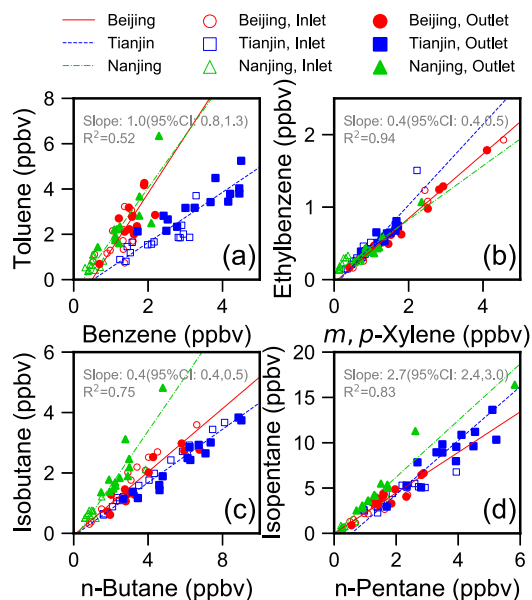


Fig. 2. Correlations between (a) toluene and benzene, (b) ethylbenzene and *m, p*-xylene, (c) isobutane and *n*-butane, and (d) isopentane and *n*-pentane in the tunnel tests (open markers: inlet, solid markers: outlet). Different colors and shapes for the markers represent different tunnel tests. Superimposed is the reduced major axis (RMA) regression line fitting to the samples (both the inlet and outlet samples in each tunnel test). The slopes and R^2 of overall regression are annotated. Results of the RMA regression in each tunnel test are listed in Table S3.

The vehicular E/X ratios (Fig. 2b) were 0.4 (95% CI: 0.4, 0.5) in Beijing, 0.6 (95% CI: 0.5, 0.7) in Tianjin, 0.4 (95% CI: 0.3, 0.4) in Nanjing and 0.4 (95% CI: 0.4, 0.5) in these three tunnel tests. Chang et al. (2006) measured an ambient E/X ratio of 0.5 (95% CI: 0.4, 0.7) in a metropolitan area. The E/X ratio is potentially utilized to estimate OH exposure ($[\text{OH}]/\Delta t$) because these two isomers most likely originate from same anthropogenic sources in a rather stable proportion but have a large difference in the reaction rates with OH (E: $7.1 \times 10^{-12} \text{ cm}^3 \text{ molecule}^{-1} \text{ s}^{-1}$; X: $18.9 \times 10^{-12} \text{ cm}^3 \text{ molecule}^{-1} \text{ s}^{-1}$) (Wang et al., 2015; Chang et al., 2006; Nelson and Quigley, 1983), leading to increased ambient E/X ratios during photochemical aging. Our tunnel tests suggested that $([\text{E}]/[\text{X}])_{t=0}$ were close to 0.4 (95% CI: 0.4, 0.5) for areas where vehicular emissions dominated total VOC emissions. The results were comparable with previous studies, which reported that the $([\text{E}]/[\text{X}])_{t=0}$ was around 0.3–0.4 for vehicular emissions (Liu et al., 2008).

The vehicular *i*-Bu/*n*-Bu ratios (Fig. 2c) were 0.6 (95% CI: 0.4, 0.6) in Beijing, 0.4 (95% CI: 0.4, 0.5) in Tianjin, 0.9 (95% CI: 0.7, 1.1) in Nanjing and 0.5 (95% CI: 0.4, 0.5) in these three tunnel tests. The lower confidence level of the *i*-Bu/*n*-Bu ratio in Nanjing (i.e., 0.7) is still higher than the upper confidence value in Beijing (i.e., 0.6) and Tianjin (i.e., 0.5), implying that the *i*-Bu/*n*-Bu ratio in Nanjing was significantly higher than that in Beijing and Tianjin. In addition, the *i*-Bu/*n*-Bu ratios measured in the Beijing and Tianjin tunnels were comparable with those for GV sources (i.e., 0.6–0.7) (Liu et al., 2008), while the *i*-Bu/*n*-Bu ratio measured in the Nanjing tunnel was comparable with that for NG sources (i.e., ~0.8) (Zheng et al., 2018). Thus, a higher *i*-Bu/*n*-Bu ratio could be observed for a fleet characterized by LNG-fueled vehicles (e.g., the Nanjing tunnel) than that characterized by GVs (the Beijing and Tianjin tunnels).

The vehicular *i*-P/*n*-P ratios (Fig. 2d) were 2.2 (95% CI: 1.9, 2.7) in Beijing, 3.0 (95% CI: 2.3, 3.8) in Tianjin, 3.1 (95% CI: 2.8, 3.5) in Nanjing and 2.7 (95% CI: 2.5, 2.9) in these three tunnel tests. The *i*-P/*n*-P ratio is a useful metric for investigating the impacts of vehicular exhaust emissions versus oil and gas emissions on ambient VOCs, since vehicular exhaust emissions are more aggravated in isopentane, leading

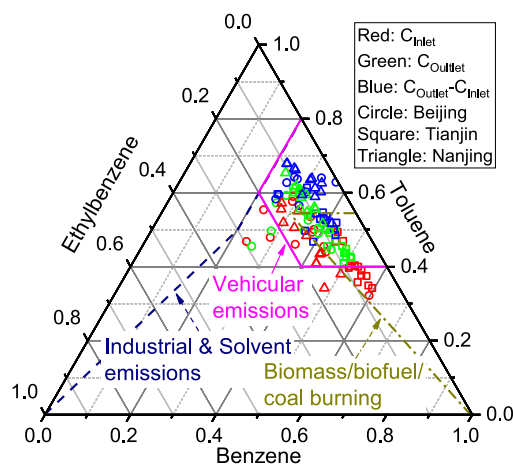


Fig. 3. Relative proportions of benzene, toluene, and ethylene from the tunnel samples. The boundary/wireframe of 'Vehicular emissions' (solid line) was defined by the 5%, 5%, and 95% percentiles of the relative proportions of benzene, toluene, and ethylbenzene from the scatters (i.e., C_{Inlet} , C_{Outlet} , and $C_{\text{Outlet}} - C_{\text{Inlet}}$) in the ternary diagram, respectively. The wireframes of 'Industrial & Solvent emissions' (dash line) and 'Biomass/biofuel/coal burning' (dash-dot line) were from Zhang et al. (2016)'s study.

to a larger *i*-P/*n*-P ratio than that from NG emissions (Thompson et al., 2014). Previous studies reported that the *i*-P/*n*-P ratio was 0.8–1.2 for NG sources (Zheng et al., 2018; Gilman et al., 2013), 2.2–3.9 for vehicular sources (Gentner et al., 2013; McGaughey et al., 2004; Hwa et al., 2002; Broderick and Marnane, 2002). In this study, the *i*-P/*n*-P ratios in the three tunnels were all within the range of the reported ratios from vehicular emissions. However, the *i*-P/*n*-P ratio in the Nanjing tunnel was unexpectedly similar with that in the Beijing and Tianjin tunnel, and different with that for raw NG sources although the Nanjing fleet comprised ~13% LNG-fueled vehicles. There are two possible explanations: the observed isopentane and *n*-pentane in the tunnels were mainly dominated by GV emissions since isopentane and *n*-pentane are abundant in both tailpipe and evaporative emissions of GVs; and the emission of LNG-fueled vehicles is different from that of raw NG sources, likely due to the combustion process in the LNG engine.

To overcome the overlapping effects of the T/B ratio among different emission sources, we used a ternary diagram of the relative compositions of B, T, and E from the tunnel samples to better distinguish vehicular emissions from other emission sources (Fig. 3) (Zhu et al., 2018; Zhang et al., 2016). On average, the B:T:E ratios of the ΔCon . were $0.32 \pm 0.08 : 0.58 \pm 0.08 : 0.10 \pm 0.05$ for the Beijing tunnel, $0.39 \pm 0.03 : 0.52 \pm 0.04 : 0.09 \pm 0.03$ for the Tianjin tunnel, $0.30 \pm 0.05 : 0.62 \pm 0.05 : 0.07 \pm 0.02$ for the Nanjing tunnel, and $0.32 \pm 0.06 : 0.59 \pm 0.06 : 0.09 \pm 0.04$ for the three tunnels. Despite the different fleet compositions, the relative compositions of B, T, and E from the tunnel samples were relatively stable and mainly concentrated within the boundary/wireframe (Fig. 3), which were defined by the 5%, 5%, and 95% percentiles of the relative proportions of B, T and E from the scatters (i.e., C_{Inlet} , C_{Outlet} , and $C_{\text{Outlet}} - C_{\text{Inlet}}$). In addition, the mean B:T:E ratio in our tunnel tests was consistent with Zhang et al. (2016)'s study with a mean B:T:E ratio of 0.31:0.59:0.10 for vehicular emissions.

3.3. Fleet-average source profiles

Fleet-average source profiles and EFs of VOCs from vehicular emissions are absolutely vital for interpreting results of receptor models for source apportionment studies and establishment of bottom-up VOC emission inventories. Compared with laboratory studies (e.g., dynamometer tests), tunnel tests provide more accurate reflection of real-world fleet emissions (including both tailpipe and evaporative

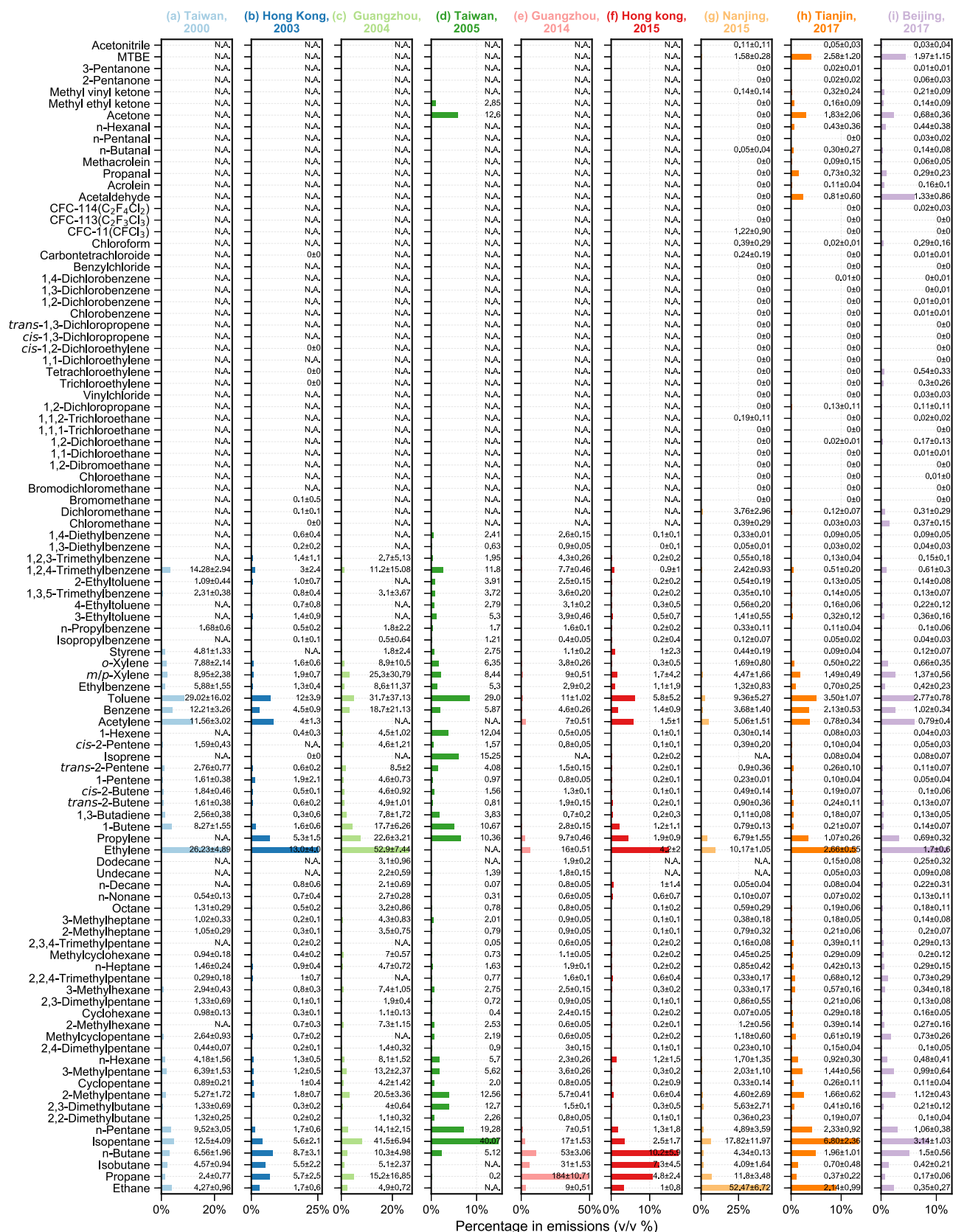


Fig. 4. Fleet-average source profiles (bar charts) and EFs ($\mu \pm \sigma$, unit: $\text{mg km}^{-1} \text{veh}^{-1}$, texts annotated on the figure) of vehicular VOC emissions in this study (i.e., Beijing in 2017: 98% GVs, Tianjin in 2017: 94% GVs, and Nanjing in 2015: 87% GVs & 13%LNG), and those from previous tunnel studies, including Taiwan in 2000 (94–98%LDV) (Hwa et al., 2002); Hong Kong in 2003 (43% GVs & 47% DVs & 10%LPG) (Ho et al., 2009); Guangzhou in 2004 (60%LDV) (Fu et al., 2005); Taiwan in 2005 (10–20%HDV) (Hung-Lung et al., 2007); Guangzhou in 2014 (61% GVs & 12% DVs & 27%LPG) (Zhang et al., 2018c); and Hong Kong in 2015 (77% GVs & 19% DVs & 3%LPG) (Cui et al., 2018). The data for this figure are listed in Tables S5–S6.

emissions). Fig. 4 presents the fleet-average source profiles and EFs of vehicular VOC emissions in this study (i.e., Beijing in 2017, Tianjin in 2017, and Nanjing in 2015), and those from previous tunnel studies, including Taiwan in 2000 (Hwa et al., 2002); Hong Kong in 2003 (Ho et al., 2009); Guangzhou in 2004 (Fu et al., 2005); Taiwan in 2005 (Hung-Lung et al., 2007); Guangzhou in 2014 (Zhang et al., 2018c); and Hong Kong in 2015 (Cui et al., 2018).

The source profile measured in the Tianjin tunnel was highly correlated (Pearson's $r = 0.90$, $p < 0.01$) with that measured in the Beijing tunnel, due to similar test year, fleet composition and fuel quality. Thus, the source profiles measured in these tunnels were most likely to be that from GVs. However, the source profile measured in the Nanjing tunnel was poorly correlated with those in either Beijing (Pearson's $r = 0.31$, $p < 0.01$) or Tianjin (Pearson's $r = 0.58$, $p < 0.01$), again indicating different VOC emission sources between the Nanjing fleet and the Beijing/Tianjin fleet. Despite these differences, the tunnel tests from 2000 to 2017 yielded some similarities in source profiles (see Fig. 4), which characterized by low-carbon alkanes (e.g., isopentane, n-pentane, n-butane, ethane, and n-butane), alkenes (e.g., ethylene and propylene), alkyne (e.g., acetylene), and aromatics (e.g., benzene and toluene).

Table S4 summarized top 5 VOC species in the source profiles (by volume) from the different tunnel studies. For fleets with overwhelming majority of GVs/LDV (e.g., Taiwan, 2000; Taiwan, 2005; Tianjin, 2017; and Beijing, 2017), ethylene, isopentane, and toluene were the most abundant species, which suggested that tailpipe emissions contributed the most to fleet emissions since those species were generally enriched in tailpipe emissions (Wang et al., 2013; Guo et al., 2011; Liu et al., 2008). Additionally, evaporative emissions were also quite common for those fleets since isopentane, the most abundant species from gasoline evaporation (Zhang et al., 2013), was frequently observed in top 5 species in tunnel tests (e.g., Taiwan, 2000; Guangzhou, 2004; Taiwan, 2005; Nanjing, 2015; Tianjin, 2017; and Beijing, 2017). Methyl *tert*-butyl ether (MTBE), an oxygenated gasoline additive to increase the octane number and reduce vehicular emissions of carbon monoxide, was abundant in Beijing and Tianjin rather than Nanjing, because MTBE is mainly present in gasoline-related emissions (Zhang et al., 2013; Pouloupoulos and Philippopoulos, 2000). Compared with the Beijing and Tianjin tunnels (Fig. 4), ethane was more enriched in the Nanjing tunnel, while propane was more enriched in the Guangzhou and Hong Kong tunnels. The results indicated that ethane and propane could be suitable tracers for LNG and LPG sources, respectively (Gilman et al., 2013; Guo et al., 2011).

3.4. Fleet-average emission factors

The average EFs for speciated VOCs and VOC groups are summarized in Fig. 4 and Table S4, respectively. The fleet-average EF of the measured VOCs in the Nanjing tunnel ($174.39 \pm 16.86 \text{ mg km}^{-1} \text{ veh}^{-1}$) was substantially higher than that in the Beijing tunnel ($33.32 \pm 2.75 \text{ mg km}^{-1} \text{ veh}^{-1}$) and the Tianjin tunnel ($45.12 \pm 10.97 \text{ mg km}^{-1} \text{ veh}^{-1}$). The difference in those EFs could be mainly ($\sim 74\%$) attributed to alkanes emissions, which were enhanced for fleets characterized by LNG-fueled vehicles. Since previous studies did not measure halocarbons and OVOCS, the fleet-average EFs of total PAMS (the 57 VOC species designated as photochemical precursors by the United States Environmental Protection Agency; including alkanes, alkenes, alkyne, and aromatics) and fractions of VOC groups in this study and previous studies were shown in Fig. 5. In general, alkanes dominated (41.3–76.2%) fleet VOC emissions (by mass) in the tunnel tests, except for a test in Taiwan in 2000 (Hwa et al., 2002). The fractions of alkanes in total VOCs in tunnel tests in Guangzhou in 2014 and in Nanjing in 2015 were much higher than the other tunnel tests, mainly due to proportions of LPG- and LNG-fueled vehicles in the fleets. Aromatics was the second largest group, and contributed 14.2–40.0% of total VOC emissions. The lowest EFs of PAMS were observed in the Beijing tunnel

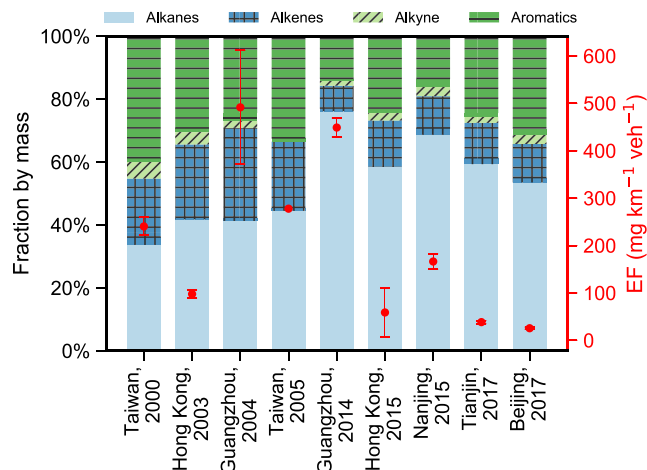


Fig. 5. Fleet-average emission factors (error bar plot, right axis) of total PAMS VOC species (the 57 VOC species designated as photochemical precursors by the United States Environmental Protection Agency; including alkanes, alkenes, alkyne, and aromatics) and fractions of VOC groups (stacked barplot, left axis) in this study and previous tunnel studies.

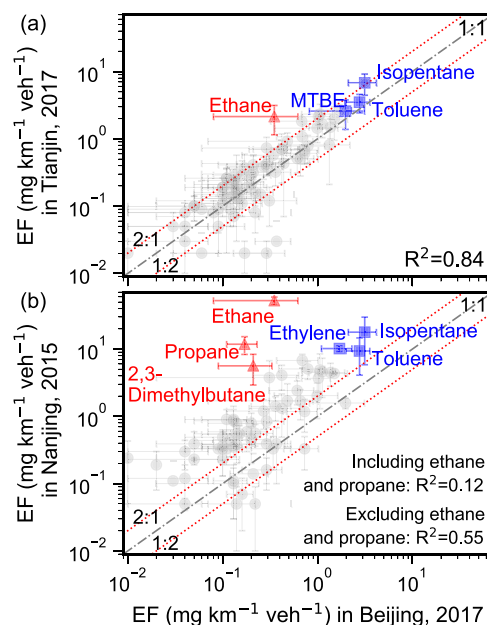


Fig. 6. Comparison of emission factors ($\mu \pm \sigma$) of speciated VOCs in (a) the Tianjin tunnel vs. Beijing tunnel, and (b) the Nanjing tunnel vs. Beijing tunnel.

($25.56 \pm 2.19 \text{ mg km}^{-1} \text{ veh}^{-1}$) and Tianjin tunnel ($38.42 \pm 3.34 \text{ mg km}^{-1} \text{ veh}^{-1}$), which were expected to be related to the lowest proportions of HDV, and the improvement of fuel quality and intensified emission standards. In addition, inconsistent EFs of VOCs in different tunnel studies were observed, mainly due to different test years, fuel types, fleet compositions, etc. However, a large difference between fleet-average VOC EFs in Guangzhou in 2014 and in Beijing in 2017 was surprisingly observed, and the difference could be as high as 16.6 times. The improvement of fuel quality from 2014 to 2017 could explain a small part of the difference, but a larger part of the difference might be explained by the different fleet compositions.

To further explore the impacts of fleet composition on fleet-average VOC EFs, the EFs of speciated VOCs in our tunnel tests were compared in Fig. 6a–b. A good correlation ($R^2 = 0.84$) between the VOC EFs in the Beijing tunnel and those in the Tianjin tunnel was found, indicating

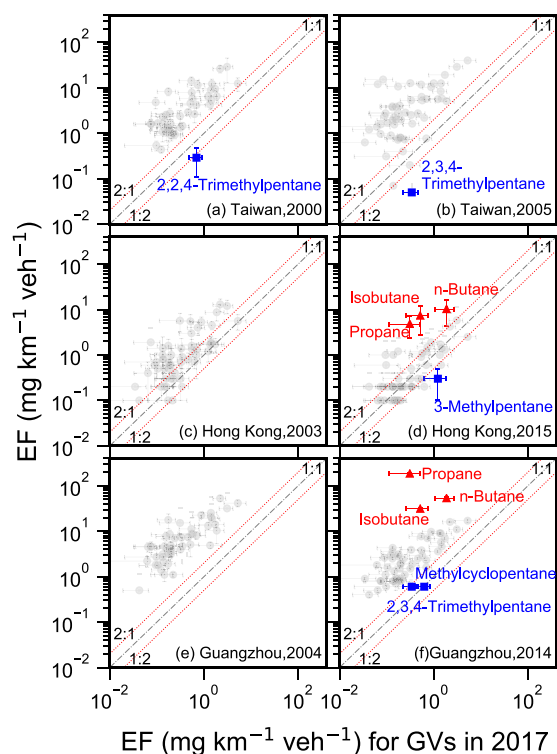


Fig. 7. Comparison of emission factors ($\mu \pm \sigma$) of speciated VOCs for gasoline vehicles (GVs) in 2017 (i.e., average EFs in the Beijing and Tianjin tunnels) and those from previous studies (Taiwan in 2000 (Hwa et al., 2002); Hong Kong in 2003 (Ho et al., 2009); Guangzhou in 2004 (Zhang et al., 2018c); Taiwan in 2005 (Hung-Lung et al., 2007); Guangzhou in 2014 (Zhang et al., 2018c); Hong Kong in 2015 (Cui et al., 2018)).

that tunnel test is a repeatable and idealized measure to estimate real-world vehicular VOC emissions. Since the Beijing fleet and Tianjin fleet both comprised >94% GV, the VOC emissions from the two fleets could generally represent those from GV. Isopentane, toluene, and MTBE (denoted in blue color in Fig. 6a) were the three most abundant VOC species in VOC emissions (by mass) from GV. The EF of ethane (denoted in red color in Fig. 6a) in Tianjin tunnel was slightly higher than that in Beijing tunnel, likely due to a proportion (i.e., $3.8 \pm 0.3\%$) of alternative-fueled vehicles (especially for CNG-fueled taxis) in the Tianjin fleet. The fleet-average VOC EFs in the Nanjing tunnel were generally higher than those in the Beijing tunnel (see Fig. 6b), and poorly correlated ($R^2 = 0.12$) with those in the Beijing tunnel, but well correlated ($R^2 = 0.55$) when excluding ethane and propane (denoted in red color in Fig. 6b). As shown in Fig. 6b, ethane, propane, and 2, 3-dimethylbutane were the key tracers that could distinguish LNG-fueled vehicles from GV. These species are by-products during processing raw natural gas and thus, enriched in VOC emissions from LNG-fueled vehicles. Isopentane, toluene, and ethylene (denoted in blue color in Fig. 6b) were the three most abundant species in VOC emissions (by mass) for both the Nanjing fleet and the Beijing fleet, due to a high proportion of GV in both fleets.

In addition, good correlations were observed between VOC EFs for GV in 2017 (defined by average EFs in the Beijing and Tianjin tunnels) and those from previous tunnel studies (see Fig. 7), suggesting that GV generally dominated fleet VOC emissions in those tunnel studies. As expected, the VOC EFs in previous studies were generally higher than those in our tunnel tests, demonstrating the effective control of vehicular VOC emissions. We also found that 2,2,4-trimethylpentane, 2,3,4-trimethylpentane, 3-methylpentane, methylcyclopentane (denoted in blue color in Fig. 7) were potential VOC tracers that could distinguish GV from other fleets. This finding was also consistent with Chang et al.

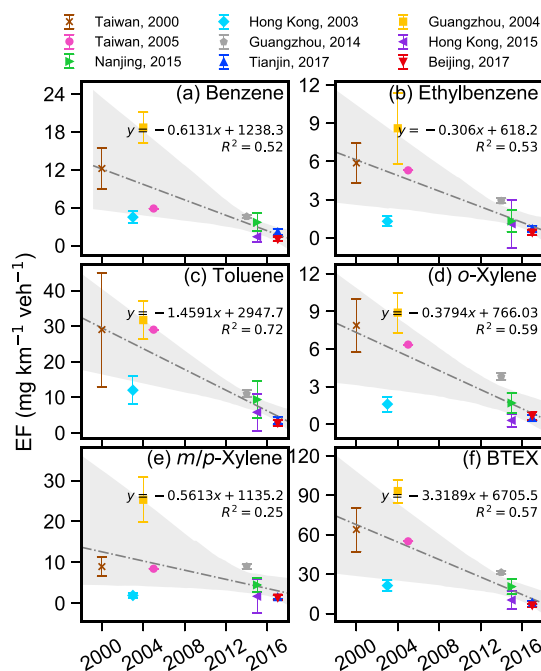


Fig. 8. Emission factors of benzene, ethylbenzene, toluene, *o*-xylene, *m, p*-xylene, and BTEX (the sum of benzene, ethylbenzene, toluene, *o*-xylene, and *m, p*-xylene) in different tunnel studies (Taiwan in 2000 (Hwa et al., 2002); Hong Kong in 2003 (Ho et al., 2009); Guangzhou in 2004 (Zhang et al., 2018c); Taiwan in 2005 (Hung-Lung et al., 2007); Guangzhou in 2014 (Zhang et al., 2018c); Nanjing in 2015 (Zhang et al., 2018a); Hong Kong in 2015 (Cui et al., 2018)), and the linear regressions (dash-dot lines filled with 95% regression confidence intervals) between the emission factors of BTEX and the test years. The slopes of the linear regressions were k values in Eq. (7).

(2006)'s study, which noted that 2,2-dimethylbutane, 3-methylpentane, methylcyclopentane, 2-methylhexane, and 3-methylhexane were potential VOC tracers for vehicular emissions since they had a good correlation with MTBE, and they are common components in both gasoline evaporation and tailpipe emissions (Doskey et al., 1999; Mugica et al., 1998). As illustrated in Fig. 7d and f, propane, isobutane, n-butane were key VOC tracers that could distinguish LPG-fueled vehicles from GV, since the fleets in the Hong Kong in 2015 and Guangzhou in 2014 comprised a large proportion of LPG-fueled vehicles.

Good correlations between the fleet-averaged VOC EFs from different tunnel tests (Fig. 8) made it possible to compare the fleet-averaged EFs measured in different years. The EFs of BTEX tested in 2014–2017 (Guangzhou in 2014, Nanjing in 2015, Hong Kong in 2015, and Tianjin in 2017) decreased dramatically (79.8% for benzene; 75.1% for toluene; 75.5% for ethylbenzene; 69.7% for *m, p*-xylene; 77.3% for *o*-xylene; and 75.3% for BTEX: the sum of benzene, toluene, ethylbenzene, *m, p*-xylene and *o*-xylene) when compared to those tested in 2000–2005 (Taiwan in 2000, Hong Kong in 2003, Guangzhou in 2004, and Taiwan in 2005), which is consistent with previous studies (Cui et al., 2018; Zhang et al., 2018c). Based on the linear regressions between the EFs of BTEX and the test years (Fig. 8), the decreased rates ($-k$ in Eq. (7), unit: $\text{mg km}^{-1} \text{veh}^{-1} \text{yr}^{-1}$) of fleet-average EFs were averaged 0.61 for benzene, 1.46 for toluene, 0.31 for ethylbenzene, 0.56 for *m, p*-xylene, 0.38 for *o*-xylene, and 3.32 for BTEX. These results again suggested the effective emission control of on-road vehicles over the last decade.

Since the 1990s, China has started vehicular emission control programs, including controls for new vehicles and in-use vehicles; improvements in fuel quality (e.g., the promotion of unleaded gasoline and low-sulfur fuels); promotion of alternative fuels and incentives for electric vehicles (Wu et al., 2017). All these strategies have been proved effective in reducing vehicular EFs (Cui et al., 2018; Zhang

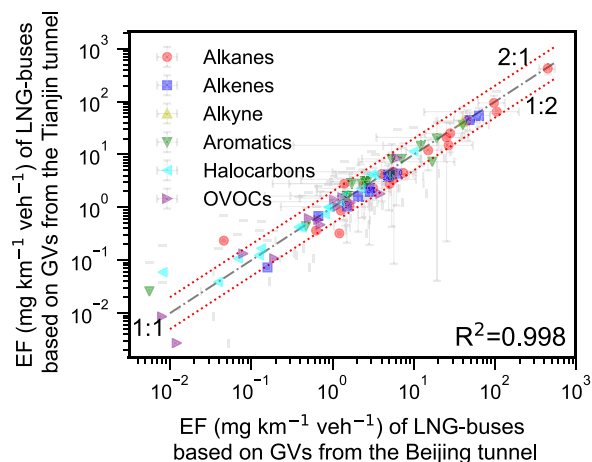


Fig. 9. Comparison of emission factors ($\mu \pm \sigma$) of speciated VOCs for LNG-buses apportioned from the Nanjing tunnel based on the emission factors of gasoline vehicles (GVs) derived from the tunnel tests in the Beijing tunnel (x-axis) and the Tianjin tunnel (y-axis).

et al., 2018a,c). According to standard GB 17930 (AQSIQ, 2017), the aromatics limit in gasoline fuel decreased only from 40% for China II-V to 35% for China VI. Therefore, the decreasing EFs of aromatics over the last decade could not be entirely attributed to the decrease of the aromatics limit in gasoline fuel, however, might be largely attributed to the improved engine technology and fuel quality. It should be noted that the fleet EFs for low-carbon alkanes (e.g., ethane and propane) will increase continuously for the foreseeable future, due to the introduction of NG/LPG-fueled taxis/buses.

3.5. VOC emissions from GVs and LNG-buses

As shown in Fig. 9, the VOC EFs for LNG-buses apportioned from the Nanjing fleet based on the EFs of GVs derived from the Tianjin tunnel, were consistent with those from the Beijing tunnel, and the R^2 of the linear regression was as high as 0.998. This satisfactory result could be explained by the similar emission nature in the Beijing tunnel and the Tianjin tunnel (see Fig. 6a). The top 3 species in VOC emissions (by weight) from LNG-buses were all alkanes (see Fig. 9), which were ethane, propane, and isopentane (in descending order). The EFs by mass (EF), volume (E_V), OFP (E_{OFP}), OH reactivity ($E_{Propy-Equiv}$) of speciated VOCs (Table S7) and VOC groups (Table S8) from GVs and LNG-buses were also reported, it should be noted that these values were average values of those calculated from the Beijing tunnel and the Tianjin tunnel.

The average EF of the measured VOCs for LNG-buses was $1113.0 \pm 381.4 \text{ mg km}^{-1} \text{ veh}^{-1}$, which was approximately 31.4 times the value of that for GVs ($35.5 \pm 13.8 \text{ mg km}^{-1} \text{ veh}^{-1}$). For chemical reactivities, the EFs by OFP and OH reactivity of the measured VOCs for LNG-buses were approximately 22.0 and 21.1 times the values of those for GVs, respectively. For the PAMS species, the estimated OFP for LNG-buses ($2497.7 \pm 1168.5 \text{ mgO}_3 \text{ km}^{-1} \text{ veh}^{-1}$) was approximately 23.4 times greater than that for GVs ($102.4 \pm 38.8 \text{ mgO}_3 \text{ km}^{-1} \text{ veh}^{-1}$). Overall, the EFs by mass, OFP, and OH reactivity for LNG-buses were 21–32 times the values of those for GVs. The much higher VOC emissions from LNG-buses were likely due to: (1) incomplete combustion due to high loads and (2) evaporative emissions of short-chain alkanes. However, the high VOC emissions from LNG-buses might be offset by their higher passenger capacity considering traffic demands given the number of passengers on an LNG-bus for a trip is 21–31 times that on a passenger car.

For GVs, alkanes contributed the most ($41.7 \pm 9.6\%$) to total VOC emissions (by volume), followed by alkenes ($19.1 \pm 5.4\%$), OVOCs

($16.2 \pm 8.9\%$), aromatics ($14.9 \pm 4.4\%$), alkyne ($4.6 \pm 5.2\%$), halocarbons ($3.5 \pm 3.3\%$). For LNG-buses, alkanes contributed as high as $75.6 \pm 5.6\%$ of total VOC emissions (by volume), followed by alkenes ($13.2 \pm 2.2\%$), alkyne (5.0 ± 2.0), aromatics (3.9 ± 3.1), halocarbons ($1.3 \pm 1.6\%$), and OVOCs ($1.0 \pm 1.9\%$). In general, alkanes constituted the largest proportion ($41.7\text{--}75.6\%$) of the EFs both by mass and by volume, from both GVs and LNG-buses. However, we still cannot conclude that alkanes dominate VOC emissions for all kind vehicle types, because alkanes contributed only $8.0\text{--}13.4\%$ to total VOC emissions for HDDVs (Mo et al., 2016; Yao et al., 2015b). A previous study noted that alkanes dominated ambient VOCs in urban areas (Song et al., 2019). Thus, the high-content alkanes in the ambient VOCs were likely due to direct emissions from gasoline and NG sources, but not from diesel sources. The proportions of alkanes in total VOCs both by mass and by volume from LNG-fueled vehicles were approximately 0.6–0.8 times greater than the values of those from GVs. For chemical reactivity, aromatics and alkenes constituted the largest proportion of both OFP and OH reactivity from gasoline- and LNG-fueled vehicles, respectively, though alkanes dominated VOC emissions from gasoline- and LNG-fueled vehicles both by mass and by volume.

For speciated VOCs ($v/v\%$, see Fig. 10a–b), ethane, isopentane, n-pentane, ethylene, propylene, acetylene, and toluene were in the top 10 species both for GVs and LNG-buses. n-Butane, acetaldehyde, and MTBE were additionally in the top 10 species for GVs, whereas propane, isobutane, and 2,3-dimethylbutane were additionally in the top 10 species for LNG-buses. Ethane and propane accounted respectively for $55.8 \pm 12.6\%$ and $8.12 \pm 2.2\%$ of the total VOCs for LNG-fueled vehicles, the fractions were ~ 8.7 times and ~ 9.0 times the values of those from GVs, which were $6.4 \pm 5.8\%$ and $0.9 \pm 0.5\%$, respectively. The results suggested that ethane and propane are more enriched in LNG-fueled vehicles than in GVs. MTBE was exclusively observed ($3.9 \pm 1.5\%$) in VOC emissions from GVs, indicating MTBE is a key tracer to differentiate GVs and LNG-fueled vehicles. The volume fraction of isobutane ($1.2 \pm 0.4\%$) was lower than that of n-butane ($4.3 \pm 1.3\%$) for GVs. However, the volume fraction of isobutane ($1.7 \pm 0.7\%$) was higher than that of n-butane ($0.9 \pm 0.4\%$) for LNG-buses. Consequently, the $i\text{-Bu}/n\text{-Bu}$ ratio could be applied as a diagnostic ratio to distinguish VOC emissions from gasoline- ($i\text{-Bu}/n\text{-Bu} < 1$) and LNG ($i\text{-Bu}/n\text{-Bu} > 1$)-fueled vehicles.

For source profiles of VOC emissions by OFP ($wt\%$, see Fig. 10c–d), isopentane, ethylene, propylene, *trans*-2-butene, toluene, *m,p*-xylene, and 1,2,4-trimethylbenzene were in the top 10 species for both gasoline- and LNG-fueled vehicles. *O*-xylene, acetaldehyde, and propanal were additionally observed in the top 10 species for GVs, whereas ethane, *trans*-2-pentene, and 3-ethyltoluene were additionally observed in the top 10 species for LNG-fueled vehicles. Therefore, control of the contents of ethylene, *m,p*-xylene, and toluene in gasoline might be beneficial for decreasing OFP from GVs. In addition, control of the contents of ethylene, propylene, and *m,p*-xylene might be beneficial for decreasing the OFP from LNG-fueled vehicles.

For source profiles of VOC emissions by OH reactivity ($v/v\%$, see Fig. 10e–f), isopentane, ethylene, propylene, *trans*-2-butene, *trans*-2-pentane, toluene, *m,p*-xylene, and 1,2,4-trimethylbenzene were in the top 10 species for both gasoline- and LNG-fueled vehicles. Acetaldehyde and n-hexanal were additionally observed in the top 10 species for GVs, whereas 2,3-dimethylbutane and acetylene were additionally observed in the top 10 species for LNG-fueled vehicles. Propylene and ethylene constituted the largest proportions (i.e., $18.8 \pm 4.8\%$ and $8.9 \pm 3.0\%$ for GVs, respectively; $21.5 \pm 6.6\%$ and $9.5 \pm 3.7\%$ for LNG-buses, respectively) of OH reactivity for both gasoline- and LNG-fueled vehicles. Control of the contents of ethylene and propylene might be beneficial for decreasing OFP and OH reactivity for both gasoline- and LNG-fueled vehicles.

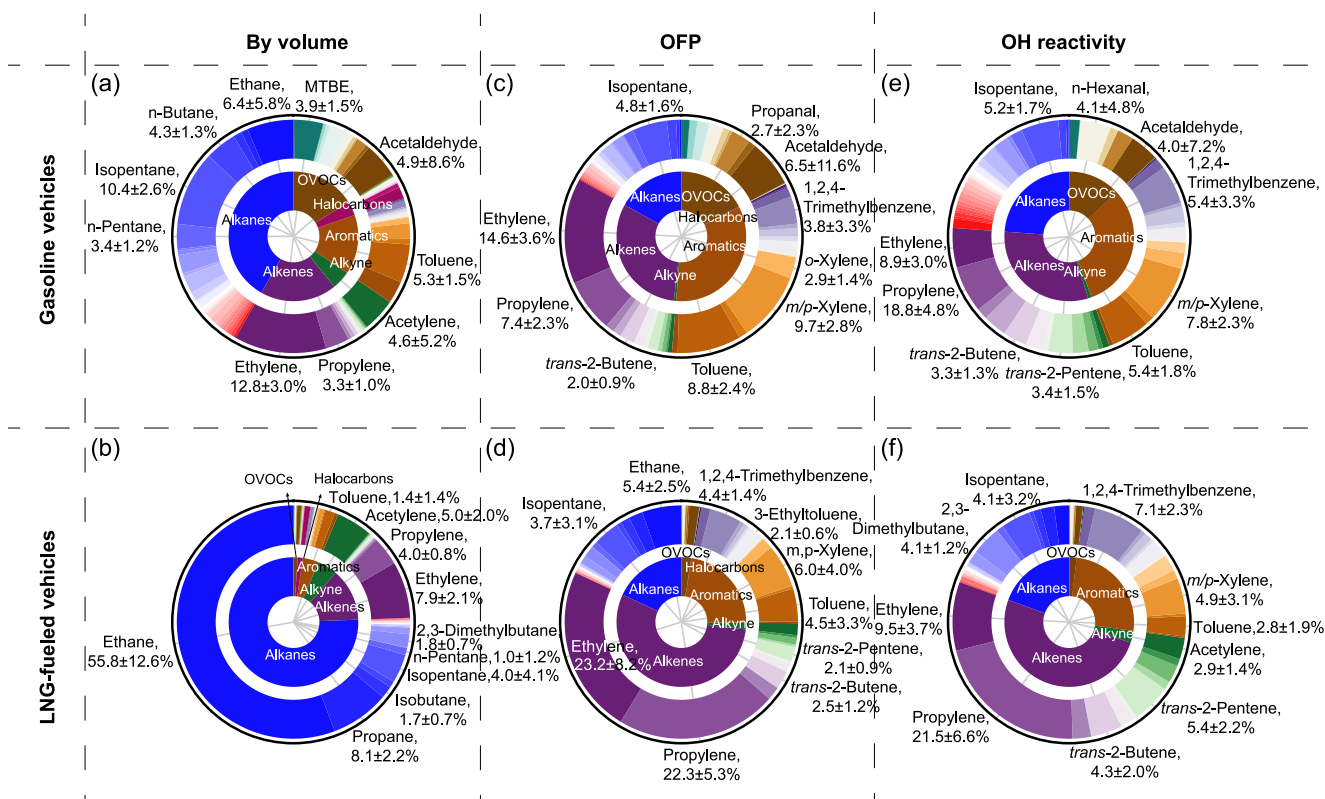


Fig. 10. Source profiles and top 10 species of VOC emissions by volume, ozone formation potential (OFF) and OH reactivity from gasoline- and LNG-fueled vehicles. The inner circle is for the VOC groups, and the outer circle is for the measure 99 VOC species (the counter-clockwise is the species from the bottom to upper in Fig. 4). The data for this figure are listed in Tables S7–S8.

3.6. Uncertainty and limitation

Several limitations should be noted in this study. Firstly, the Beijing and Tianjin fleets in 2017 still comprised a very small proportion of vehicles powered by diesel and alternative-fuel, though the hourly proportion of these vehicles never exceeded 10% during the tunnel tests. Therefore, the fleet-average EFs and source profiles in the Beijing and Tianjin tunnels were not completely from GVs. However, the proportions of GVs in the Beijing (~98%) and Tianjin (~94%) fleets were so far the highest compared with previous studies. Secondly, the tunnel test in the Nanjing tunnel is two years before those in the Beijing and Tianjin tunnels. Despite we estimated the EFs of VOCs from GV in 2015 by measurements in 2017, the fleet average source profile of VOCs from GVs might have changed a little due to rapid upgrading of fuel quality in China. Thirdly, the tunnel tests in the three urban tunnels were all conducted at ambient temperature higher than 20 °C, which would be problematical since VOCs emissions from tailpipe decrease with temperature (George et al., 2015, 2017) while evaporative emissions increase with temperature (Rubin et al., 2006). Song et al. (2019) noted that the response of real-world vehicular VOC emissions on temperature exhibited a V-shape pattern, implying dynamic VOC EFs due to comprehensive effects of temperature dependence of tailpipe and evaporative VOC emissions. Thus, the EFs derived in this study should be carefully adjusted based on the response of vehicular VOC emissions on temperature. Future studies should focus on long-term tunnel tests to offer more accurate estimation of real-world VOC emissions from on-road vehicles.

4. Conclusions

The measurement of fleet-average VOC source profiles and emission factors through tunnel tests is resource intensive. There have been few studies in which fleet emissions were apportioned to fuel-specific

vehicle types using multiple tunnel tests. Here, we reported in-depth analysis of an extensive dataset of VOC samples collected in three urban tunnels in China, and comparison of VOC emissions from gasoline and LNG-fueled vehicles.

The EFs of speciated VOCs in the Tianjin tunnel were highly correlated with those in the Beijing tunnel implied that tunnel test is an idealized measure to estimate real-world vehicular VOC emissions. The fleet-average EF of the measured VOCs in the Nanjing tunnel was 3.9–5.2 times that in the Beijing tunnel and the Tianjin tunnel, largely (~74%) due to alkanes emissions from LNG-fueled vehicles. The results demonstrated that inconsistent fleet-average VOC emissions could be largely explained by different fleet compositions. The characteristic ratios for vehicular emissions were 1.0 (95% CI: 0.8, 1.3) for T/B, 0.4 (95% CI: 0.4, 0.5) for E/X, (95% CI: 0.4, 0.5) for *i*-Bu/*n*-Bu, (95% CI: 2.5, 2.9) for *i*-P/*n*-P, and $0.32 \pm 0.06:0.59 \pm 0.06:0.09 \pm 0.04$ for B:T:E. VOC emissions from LNG/LPG-fueled vehicles can be differentiated from GVs through multiple tunnel tests using constrained linear regression. The VOC EFs by mass, OFF, and OH reactivity for LNG-buses were approximately 21.1–31.4 times the values of those for GVs. Our work could be beneficial for interpreting results of receptor models for VOC source apportionment studies, and establishment of bottom-up VOC emission inventories.

CRedit authorship contribution statement

Congbo Song: Data curation, Formal analysis, Investigation, Methodology, Visualization, Writing - original draft, Writing - review & editing. **Yan Liu:** Data curation, Investigation, Writing - review & editing. **Luna Sun:** Data curation, Investigation. **Qijun Zhang:** Data curation, Investigation. **Hongjun Mao:** Conceptualization, Funding acquisition, Supervision, Writing - review & editing.

Declaration of competing interest

The authors declare that they have no known competing financial interests or personal relationships that could have appeared to influence the work reported in this paper.

Acknowledgments

This work was funded by the National Key Research and Development Program of China (2017YFC0212100), the Key Technologies R & D Program of Tianjin (19YFZCSF00960), and the National Natural Science Foundation of China (No. 41705080). The authors acknowledge all members of Center for Urban Transport Emission Research (CUTER), Tianjin Vehicle Emission Control Joint Laboratory, China Waterborne Transport Research Institute, and management offices of the tunnels for their support and help during the sampling campaigns. The authors also would like to thank the editor and reviewers for their thoughtful comments and efforts towards improving our manuscript. The authors are extremely grateful to the authors that contributed to the existing tunnel tests, which make the inter-comparison of different studies possible.

Appendix A. Supplementary data

Supplementary material related to this article can be found online at <https://doi.org/10.1016/j.atmosenv.2020.117626>.

References

- AQSIQ, 2017. GB17930-2016: Gasoline for motor vehicles. URL: <https://www.vecc.org.cn/xgbzyp/2324.jhtml> [Chinese, last access: 24 May 2020].
- Atkinson, R., Arey, J., 2003. Atmospheric degradation of volatile organic compounds. *Chem. Rev.* 103 (12), 4605–4638. <http://dx.doi.org/10.1021/cr0206420>.
- Broderick, B., Marnane, I., 2002. A comparison of the c2–c9 hydrocarbon compositions of vehicle fuels and urban air in dublin, Ireland. *Atmos. Environ.* 36 (6), 975–986. [http://dx.doi.org/10.1016/S1352-2310\(01\)00472-1](http://dx.doi.org/10.1016/S1352-2310(01)00472-1).
- Brown, S.G., Frankel, A., Hafner, H.R., 2007. Source apportionment of vocs in the los angeles area using positive matrix factorization. *Atmos. Environ.* 41 (2), 227–237. <http://dx.doi.org/10.1016/j.atmosenv.2006.08.021>.
- Cao, X., Yao, Z., Shen, X., Ye, Y., Jiang, X., 2016. On-road emission characteristics of vocs from light-duty gasoline vehicles in Beijing, China. *Atmos. Environ.* 124, 146–155. <http://dx.doi.org/10.1016/j.atmosenv.2015.06.019>.
- Carter, W.P., 1994. Development of ozone reactivity scales for volatile organic compounds. *Air Waste* 44 (7), 881–899. <http://dx.doi.org/10.1080/1073161X.1994.10467290>.
- Chang, C.-C., Wang, J.-L., Liu, S.-C., Lung, S.-C.C., 2006. Assessment of vehicular and non-vehicular contributions to hydrocarbons using exclusive vehicular indicators. *Atmos. Environ.* 40 (33), 6349–6361. <http://dx.doi.org/10.1016/j.atmosenv.2006.05.043>.
- Chen, F., Hu, W., Zhong, Q., 2013. Emissions of particle-phase polycyclic aromatic hydrocarbons (pahs) in the fu gui-shan tunnel of nanjing, China. *Atmos. Res.* 124, 53–60. <http://dx.doi.org/10.1016/j.jatmosres.2012.12.008>.
- Colberg, C.A., Tona, B., Catone, G., Sangiorgio, C., Stahel, W.A., Sturm, P., Staehelin, J., 2005. Statistical analysis of the vehicle pollutant emissions derived from several european road tunnel studies. *Atmos. Environ.* 39 (13), 2499–2511. <http://dx.doi.org/10.1016/j.atmosenv.2004.07.037>.
- Cui, M., Chen, Y., Tian, C., Zhang, F., Yan, C., Zheng, M., 2016. Chemical composition of pm_{2.5} from two tunnels with different vehicular fleet characteristics. *Sci. Total Environ.* 550, 123–132. <http://dx.doi.org/10.1016/j.scitotenv.2016.01.077>.
- Cui, L., Wang, X.L., Ho, K.F., Gao, Y., Liu, C., Ho, S.S.H., Li, H.W., Lee, S.C., Wang, X.M., Jiang, B.Q., Huang, Y., Chow, J.C., Watson, J.G., Chen, L.-W., 2018. Decrease of voc emissions from vehicular emissions in Hong Kong from 2003 to 2015: Results from a tunnel study. *Atmos. Environ.* 177, 64–74. <http://dx.doi.org/10.1016/j.atmosenv.2018.01.020>.
- Dodge, M.C., 1984. Combined effects of organic reactivity and nmhc/nox ratio on photochemical oxidant formation—a modeling study. *Atmos. Environ.* 18 (8), 1657–1665. [http://dx.doi.org/10.1016/0004-6981\(84\)90388-3](http://dx.doi.org/10.1016/0004-6981(84)90388-3).
- Doskey, P.V., Fukui, Y., Sultan, M., Maghraby, A.A., Taher, A., 1999. Source profiles for nonmethane organic compounds in the atmosphere of Cairo, Egypt. *J. Air Waste Manag. Assoc.* 49 (7), 814–822. <http://dx.doi.org/10.1080/10473289.1999.10463850>.
- Fang, X., Wu, L., Zhang, Q., Zhang, J., Wang, A., Zhang, Y., Zhao, J., Mao, H., 2019. Characteristics, emissions and source identifications of particle polycyclic aromatic hydrocarbons from traffic emissions using tunnel measurement. *Transp. Res. Part D: Transp. Environ.* 67, 674–684. <http://dx.doi.org/10.1016/j.trd.2018.02.021>.
- Fu, L., Shao, M., Liu, Y., Liu, Y., Lu, S., Tang, D., 2005. Tunnel experimental study on the emission factors of volatile organic compounds (vocs) from vehicles. *Huanjing Kexue Xuebao/Acta Sci. Circumstantiae* 25 (7), 879–885. <http://dx.doi.org/10.3321/j.issn:0253-2468.2005.07.004>, [Chinese].
- Gentner, D.R., Worton, D.R., Isaacman, G., Davis, L.C., Dallmann, T.R., Wood, E.C., Herndon, S.C., Goldstein, A.H., Harley, R.A., 2013. Chemical composition of gas-phase organic Carbon emissions from motor vehicles and implications for ozone production. *Environ. Sci. Technol.* 47 (20), 11837–11848. <http://dx.doi.org/10.1021/es401470e>.
- George, L.J., Hays, M.D., Herrington, J.S., Preston, W., Snow, R., Faircloth, J., George, B.J., Long, T., Baldauf, R.W., 2015. Effects of cold temperature and ethanol content on voc emissions from light-duty gasoline vehicles. *Environ. Sci. Technol.* 49 (21), 13067–13074. <http://dx.doi.org/10.1021/acs.est.5b04102>.
- George, L., Hays, M., Snow, R., Faircloth, J., Long, T., Baldauf, R., 2017. Cold temperature effects on speciated voc emissions from modern gdi light-duty vehicles: Preliminary results. In: Emissions Inventory Conference. Baltimore, MD, URL: https://www.epa.gov/sites/production/files/2017-11/documents/cold_temperature.pdf.
- Gertler, A.W., Fujita, E.M., Pierson, W.R., Wittorff, D.N., 1996. Apportionment of nmhc tailpipe vs non-tailpipe emissions in the fort mchenry and tuscarora mountain tunnels. *Atmos. Environ.* 30 (12), 2297–2305. [http://dx.doi.org/10.1016/1352-2310\(95\)00090-9](http://dx.doi.org/10.1016/1352-2310(95)00090-9).
- Gilman, J.B., Lerner, B.M., Kuster, W.C., de Gouw, J.A., 2013. Source signature of volatile organic compounds from oil and natural gas operations in northeastern colorado. *Environ. Sci. Technol.* 47 (3), 1297–1305. <http://dx.doi.org/10.1021/es304119a>.
- Guo, H., Zou, S., Tsai, W., Chan, L., Blake, D., 2011. Emission characteristics of nonmethane hydrocarbons from private cars and taxis at different driving speeds in Hong Kong. *Atmos. Environ.* 45 (16), 2711–2721. <http://dx.doi.org/10.1016/j.atmosenv.2011.02.053>.
- Hampton, C.V., Pierson, W.R., Harvey, T.M., Schuetzle, D., 1983. Hydrocarbon gases emitted from vehicles on the road. 2. determination of emission rates from diesel and spark-ignition vehicles. *Environ. Sci. Technol.* 17 (12), 699–708. <http://dx.doi.org/10.1021/es00118a003>.
- Hampton, C.V., Pierson, W.R., Harvey, T.M., Updegrave, W.S., Marano, R.S., 1982. Hydrocarbon gases emitted from vehicles on the road. 1. A qualitative gas chromatography/mass spectrometry survey. *Environ. Sci. Technol.* 16 (5), 287–298. <http://dx.doi.org/10.1021/es00099a011>.
- Hedberg, E., Kristensson, A., Ohlsson, M., Johansson, C., Johansson, P.-Å., Swietlicki, E., Vesely, V., Wideqvist, U., Westerholm, R., 2002. Chemical and physical characterization of emissions from birch wood combustion in a wood stove. *Atmos. Environ.* 36 (30), 4823–4837. [http://dx.doi.org/10.1016/S1352-2310\(02\)00417-X](http://dx.doi.org/10.1016/S1352-2310(02)00417-X).
- Ho, K.F., Lee, S.C., Ho, W.K., Blake, D.R., Cheng, Y., Li, Y.S., Ho, S.S.H., Fung, K., Louie, P.K.K., Park, D., 2009. Vehicular emission of volatile organic compounds (vocs) from a tunnel study in Hong Kong. *Atmos. Chem. Phys.* 9 (19), 7491–7504. <http://dx.doi.org/10.5194/acp-9-7491-2009>.
- Huang, Y., Ling, Z.H., Lee, S.C., Ho, S.S.H., Cao, J.J., Blake, D.R., Cheng, Y., Lai, S.C., Ho, K.F., Gao, Y., Cui, L., Louie, P.K., 2015. Characterization of volatile organic compounds at a roadside environment in Hong Kong: An investigation of influences after air pollution control strategies. *Atmos. Environ.* 122, 809–818. <http://dx.doi.org/10.1016/j.atmosenv.2015.09.036>.
- Hung-Lung, C., Ching-Shyung, H., Shih-Yu, C., Ming-Ching, W., Sen-Yi, M., Yao-Sheng, H., 2007. Emission factors and characteristics of criteria pollutants and volatile organic compounds (vocs) in a freeway tunnel study. *Sci. Total Environ.* 381 (1), 200–211. <http://dx.doi.org/10.1016/j.scitotenv.2007.03.039>.
- Hwa, M.-Y., Hsieh, C.-C., Wu, T.-C., Chang, L.-F.W., 2002. Real-world vehicle emissions and vocs profile in the taipei tunnel located at Taiwan taipei area. *Atmos. Environ.* 36 (12), 1993–2002. [http://dx.doi.org/10.1016/S1352-2310\(02\)00148-6](http://dx.doi.org/10.1016/S1352-2310(02)00148-6).
- Khoder, M., 2007. Ambient levels of volatile organic compounds in the atmosphere of greater Cairo. *Atmos. Environ.* 41 (3), 554–566. <http://dx.doi.org/10.1016/j.atmosenv.2006.08.051>.
- Legreid, G., Reimann, S., Steinbacher, M., Staehelin, J., Young, D., Stemmler, K., 2007. ‘Measurements of ovocs and nmhcs in a swiss highway tunnel for estimation of road transport emissions. *Environ. Sci. Technol.* 41 (20), 7060–7066. <http://dx.doi.org/10.1021/es062309+>.
- Li, B., Ho, S.S.H., Xue, Y., Huang, Y., Wang, L., Cheng, Y., Dai, W., Zhong, H., Cao, J., Lee, S., 2017. Characterizations of volatile organic compounds (vocs) from vehicular emissions at roadside environment: The first comprehensive study in northwestern China. *Atmos. Environ.* 161, 1–12. <http://dx.doi.org/10.1016/j.atmosenv.2017.04.029>.
- Liu, B., Liang, D., Yang, J., Dai, Q., Bi, X., Feng, Y., Yuan, J., Xiao, Z., Zhang, Y., Xu, H., 2016. Characterization and source apportionment of volatile organic compounds based on 1-year of observational data in tianjin, China. *Environmental Pollution* 218, 757–769. <http://dx.doi.org/10.1016/j.envpol.2016.07.072>.
- Liu, Y., Shao, M., Fu, L., Lu, S., Zeng, L., Tang, D., 2008. Source profiles of volatile organic compounds (vocs) measured in China: Part I. *Atmos. Environ.* 42 (25), 6247–6260. <http://dx.doi.org/10.1016/j.atmosenv.2008.01.070>.
- Man, H., Liu, H., Niu, H., Wang, K., Deng, F., Wang, X., Xiao, Q., Hao, J., 2020. Vocs evaporative emissions from vehicles in China: Species characteristics of different emission processes. *Environ. Sci. Ecotechnol.* 1, 100002. <http://dx.doi.org/10.1016/j.jese.2019.100002>.

- McGaughey, G.R., Desai, N.R., Allen, D.T., Seila, R.L., Lonneman, W.A., Fraser, M.P., Harley, R.A., Pollack, A.K., Ivy, J.M., Price, J.H., 2004. Analysis of motor vehicle emissions in a houston tunnel during the texas air quality study 2000. *Atmos. Environ.* 38 (20), 3363–3372. <http://dx.doi.org/10.1016/j.atmosenv.2004.03.006>.
- MEEPRC, 2019. China mobile source environmental management annual report. URL: <http://www.mee.gov.cn/hjzl/sthjzk/ydyhjgl/201909/P020190905586230826402.pdf> [Chinese, last access: 24 May 2020].
- Mo, Z., Shao, M., Lu, S., 2016. Compilation of a source profile database for hydrocarbon and ovoc emissions in China. *Atmos. Environ.* 143, 209–217. <http://dx.doi.org/10.1016/j.atmosenv.2016.08.025>.
- Mugica, V., Vega, E., Arriaga, J.L., Ruiz, M.E., 1998. Determination of motor vehicle profiles for non-methane organic compounds in the Mexico city metropolitan area. *J. Air Waste Manag. Assoc.* 48 (11), 1060–1068. <http://dx.doi.org/10.1080/10473289.1998.10463770>.
- Nelson, P., Quigley, S., 1983. The *m,p*-xylenes:ethylbenzene ratio. a technique for estimating hydrocarbon age in ambient atmospheres. *Atmos. Environ.* (1967) 17 (3), 659–662. [http://dx.doi.org/10.1016/0004-6981\(83\)90141-5](http://dx.doi.org/10.1016/0004-6981(83)90141-5).
- Parrish, D.D., Kuster, W.C., Shao, M., Yokouchi, Y., Kondo, Y., Goldan, P.D., de Gouw, J.A., Koike, M., Shirai, T., 2009. Comparison of air pollutant emissions among mega-cities. *Atmos. Environ.* 43 (40), 6435–6441. <http://dx.doi.org/10.1016/j.atmosenv.2009.06.024>.
- Pierson, W.R., Brachaczek, W.W., 1983. Emissions of ammonia and amines from vehicles on the road. *Environ. Sci. Technol.* 17 (12), 757–760. <http://dx.doi.org/10.1021/es00118a013>.
- Pierson, W.R., Gertler, A.W., Robinson, N.F., Sagebiel, J.C., Zielinska, B., Bishop, G.A., Stedman, D.H., Zweidinger, R.B., Ray, W.D., 1996. Real-world automotive emissions—Summary of studies in the fort mchenry and tuscarora mountain tunnels. *Atmos. Environ.* 30 (12), 2233–2256. [http://dx.doi.org/10.1016/1352-2310\(95\)00276-6](http://dx.doi.org/10.1016/1352-2310(95)00276-6).
- Pierson, W.R., Gorse, R.A., Szkarlat, A.C., Brachaczek, W.W., Japar, S.M., Lee, F.S.C., Zweidinger, R.B., Claxton, L.D., 1983. Mutagenicity and chemical characteristics of carbonaceous particulate matter from vehicles on the road. *Environ. Sci. Technol.* 17 (1), 31–44. <http://dx.doi.org/10.1021/es00107a009>.
- Pouloupoulos, S., Philippopoulos, C., 2000. Influence of mtbe addition into gasoline on automotive exhaust emissions. *Atmos. Environ.* 34 (28), 4781–4786. [http://dx.doi.org/10.1016/S1352-2310\(00\)00257-0](http://dx.doi.org/10.1016/S1352-2310(00)00257-0).
- Rubin, J.I., Kean, A.J., Harley, R.A., Millet, D.B., Goldstein, A.H., 2006. Temperature dependence of volatile organic compound evaporative emissions from motor vehicles. *J. Geophys. Res.: Atmos.* 111 (D3), <http://dx.doi.org/10.1029/2005JD006458>.
- Schmitz, T., Hassel, D., Weber, F.-J., 2000. Determination of voc-components in the exhaust of gasoline and diesel passenger cars. *Atmos. Environ.* 34 (27), 4639–4647. [http://dx.doi.org/10.1016/S1352-2310\(00\)00303-4](http://dx.doi.org/10.1016/S1352-2310(00)00303-4).
- Song, C., Liu, B., Dai, Q., Li, H., Mao, H., 2019. Temperature dependence and source apportionment of volatile organic compounds (vocs) at an urban site on the north China plain. *Atmos. Environ.* 207, 167–181. <http://dx.doi.org/10.1016/j.atmosenv.2019.03.030>.
- Song, C., Ma, C., Zhang, Y., Wang, T., Wu, L., Wang, P., Liu, Y., Li, Q., Zhang, J., Dai, Q., Zou, C., Sun, L., Mao, H., 2018. Heavy-duty diesel vehicles dominate vehicle emissions in a tunnel study in northern China. *Sci. Total Environ.* 637–638, 431–442. <http://dx.doi.org/10.1016/j.scitotenv.2018.04.387>.
- Steinbacher, M., Dommen, J., Ordonez, C., Reimann, S., GrÜebler, F.C., Staehelin, J., Prevot, A.S.H., 2005. Volatile organic compounds in the po basin. part a: Anthropogenic vocs. *J. Atmos. Chem.* 51 (3), 271–291. <http://dx.doi.org/10.1007/s10874-005-3576-1>.
- Stemmler, K., Bugmann, S., Buchmann, B., Reimann, S., Staehelin, J., 2005. Large decrease of voc emissions of Switzerland's car fleet during the past decade: results from a highway tunnel study. *Atmos. Environ.* 39 (6), 1009–1018. <http://dx.doi.org/10.1016/j.atmosenv.2004.10.010>.
- Sun, S., Zhao, G., Wang, T., Jin, J., Wang, P., Lin, Y., Li, H., Ying, Q., Mao, H., 2019. Past and future trends of vehicle emissions in tianjin, China, from 2000 to 2030. *Atmos. Environ.* 209, 182–191. <http://dx.doi.org/10.1016/j.atmosenv.2019.04.016>.
- Thompson, C.R., Hueber, J., Helmig, D., 2014. Influence of oil and gas emissions on ambient atmospheric non-methane hydrocarbons in residential areas of northeastern colorado. *Elem. Sci. Anth.* 3, <http://dx.doi.org/10.12952/journal.elementa.000035>.
- Vega, E., Mugica, V., Carmona, R., Valencia, E., 2000. Hydrocarbon source apportionment in Mexico city using the chemical mass balance receptor model. *Atmos. Environ.* 34 (24), 4121–4129. [http://dx.doi.org/10.1016/S1352-2310\(99\)00496-3](http://dx.doi.org/10.1016/S1352-2310(99)00496-3).
- Wang, J.M., Jeong, C.-H., Hilker, N., Shairsingh, K.K., Healy, R.M., Sofowote, U., Deboz, J., Su, Y., McGaughey, M., Doerksen, G., Munoz, T., White, L., Herod, D., Evans, G.J., 2018. Near-road air pollutant measurements: Accounting for inter-site variability using emission factors. *Environ. Sci. Technol.* 52 (16), 9495–9504. <http://dx.doi.org/10.1021/acs.est.8b01914>.
- Wang, J., Jin, L., Gao, J., Shi, J., Zhao, Y., Liu, S., Jin, T., Bai, Z., Wu, C.-Y., 2013. Investigation of speciated voc in gasoline vehicular exhaust under ece and eudc test cycles. *Sci. Total Environ.* 445–446, 110–116. <http://dx.doi.org/10.1016/j.scitotenv.2012.12.044>.
- Wang, M., Li, S., Zhu, R., Zhang, R., Zu, L., Wang, Y., Bao, X., 2020. On-road tailpipe emission characteristics and ozone formation potentials of vocs from gasoline, diesel and liquefied petroleum gas fueled vehicles. *Atmos. Environ.* 223, 117294. <http://dx.doi.org/10.1016/j.atmosenv.2020.117294>.
- Wang, H., Wang, Q., Chen, J., Chen, C., Huang, C., Qiao, L., Lou, S., Lu, J., 2015. Do vehicular emissions dominate the source of c6-c8 aromatics in the megacity shanghai of eastern China?. *J. Environ. Sci.* 27, 290–297. <http://dx.doi.org/10.1016/j.jes.2014.05.033>.
- Wu, Y., Zhang, S., Hao, J., Liu, H., Wu, X., Hu, J., Walsh, M.P., Wallington, T.J., Zhang, K.M., Stevanovic, S., 2017. On-road vehicle emissions and their control in China: A review and outlook. *Sci. Total Environ.* 574, 332–349. <http://dx.doi.org/10.1016/j.scitotenv.2016.09.040>.
- Yamada, H., 2013. Contribution of evaporative emissions from gasoline vehicles toward total voc emissions in Japan. *Sci. Total Environ.* 449, 143–149. <http://dx.doi.org/10.1016/j.scitotenv.2013.01.045>.
- Yao, Z., Shen, X., Ye, Y., Cao, X., Jiang, X., Zhang, Y., He, K., 2015a. On-road emission characteristics of vocs from diesel trucks in Beijing, China. *Atmos. Environ.* 103, 87–93. <http://dx.doi.org/10.1016/j.atmosenv.2014.12.028>.
- Yao, Z., Wu, B., Shen, X., Cao, X., Jiang, X., Ye, Y., He, K., 2015b. On-road emission characteristics of vocs from rural vehicles and their ozone formation potential in Beijing, China. *Atmos. Environ.* 105, 91–96. <http://dx.doi.org/10.1016/j.atmosenv.2015.01.054>.
- Yuan, B., Shao, M., Gouw, J., Parrish, D.D., Lu, S., Wang, M., Zeng, L., Zhang, Q., Song, Y., Zhang, J., Hu, M., 2012. Volatile organic compounds (vocs) in urban air: How chemistry affects the interpretation of positive matrix factorization (pmf) analysis. *J. Geophys. Res.: Atmos.* 117 (D24), <http://dx.doi.org/10.1029/2012JD018236>.
- Yue, T., Yue, X., Chai, F., Hu, J., Lai, Y., He, L., Zhu, R., 2017. Characteristics of volatile organic compounds (vocs) from the evaporative emissions of modern passenger cars. *Atmos. Environ.* 151, 62–69. <http://dx.doi.org/10.1016/j.atmosenv.2016.12.008>.
- Zhang, S., Niu, T., Wu, Y., Zhang, K.M., Wallington, T.J., Xie, Q., Wu, X., Xu, H., 2018b. Fine-grained vehicle emission management using intelligent transportation system data. *Environ. Pollut.* 241, 1027–1037. <http://dx.doi.org/10.1016/j.envpol.2018.06.016>.
- Zhang, Y., Wang, X., Zhang, Z., Lü, S., Shao, M., Lee, F., Yu, J., 2013. Species profiles and normalized reactivity of volatile organic compounds from gasoline evaporation in China. *Atmos. Environ.* 79, 110–118. <http://dx.doi.org/10.1016/j.atmosenv.2013.06.029>.
- Zhang, Q., Wu, L., Fang, X., Liu, M., Zhang, J., Shao, M., Lu, S., Mao, H., 2018a. Emission factors of volatile organic compounds (vocs) based on the detailed vehicle classification in a tunnel study. *Sci. Total Environ.* 624, 878–886. <http://dx.doi.org/10.1016/j.scitotenv.2017.12.171>.
- Zhang, Y., Yang, W., Simpson, I., Huang, X., Yu, J., Huang, Z., Wang, Z., Zhang, Z., Liu, D., Huang, Z., Wang, Y., Pei, C., Shao, M., Blake, D.R., Zheng, J., Huang, Z., Wang, X., 2018c. Decadal changes in emissions of volatile organic compounds (vocs) from on-road vehicles with intensified automobile pollution control: Case study in a busy urban tunnel in south China. *Environ. Pollut.* 233, 806–819. <http://dx.doi.org/10.1016/j.envpol.2017.10.133>.
- Zhang, Z., Zhang, Y., Wang, X., Lü, S., Huang, Z., Huang, X., Yang, W., Wang, Y., Zhang, Q., 2016. Spatiotemporal patterns and source implications of aromatic hydrocarbons at six rural sites across China's developed coastal regions. *J. Geophys. Res.: Atmos.* 121 (11), 6669–6687. <http://dx.doi.org/10.1002/2016JD025115>.
- Zheng, H., Kong, S., Xing, X., Mao, Y., Hu, T., Ding, Y., Li, G., Liu, D., Li, S., Qi, S., 2018. Monitoring of volatile organic compounds (vocs) from an oil and gas station in northwest China for 1 year. *Atmos. Chem. Phys.* 18 (7), 4567–4595. <http://dx.doi.org/10.5194/acp-18-4567-2018>.
- Zhu, H., Wang, H., Jing, S., Wang, Y., Cheng, T., Tao, S., Lou, S., Qiao, L., Li, L., Chen, J., 2018. Characteristics and sources of atmospheric volatile organic compounds (vocs) along the mid-lower yangtze river in China. *Atmos. Environ.* 190, 232–240. <http://dx.doi.org/10.1016/j.atmosenv.2018.07.026>.
- Zou, Y., Deng, X.J., Zhu, D., Gong, D.C., Wang, H., Li, F., Tan, H.B., Deng, T., Mai, B.R., Liu, X.T., Wang, B.G., 2015. Characteristics of 1 year of observational data of vocs, no, and o₃ at a suburban site in guangzhou, China. *Atmos. Chem. Phys.* 15 (12), 6625–6636. <http://dx.doi.org/10.5194/acp-15-6625-2015>.